

April 2010

# Design of a Windspeed Monitoring System for Autonomously Guided Cargo Parachutes

Daniel Morgan Herzberg  
*Worcester Polytechnic Institute*

Joel Benjamin Altman  
*Worcester Polytechnic Institute*

Nicholas Andrew Wheeler  
*Worcester Polytechnic Institute*

Samuel Jamieson Corner  
*Worcester Polytechnic Institute*

Follow this and additional works at: <https://digitalcommons.wpi.edu/mqp-all>

---

## Repository Citation

Herzberg, D. M., Altman, J. B., Wheeler, N. A., & Corner, S. J. (2010). *Design of a Windspeed Monitoring System for Autonomously Guided Cargo Parachutes*. Retrieved from <https://digitalcommons.wpi.edu/mqp-all/527>

This Unrestricted is brought to you for free and open access by the Major Qualifying Projects at Digital WPI. It has been accepted for inclusion in Major Qualifying Projects (All Years) by an authorized administrator of Digital WPI. For more information, please contact [digitalwpi@wpi.edu](mailto:digitalwpi@wpi.edu).



Design of a Windspeed Monitoring System for Autonomously-Guided Cargo

Parachutes

A Major Qualifying Project report submitted to the Faculty of

WORCESTER POLYTECHNIC INSTITUTE

In partial fulfillment of the requirements for the degree of

Bachelor of Science in Aerospace Engineering

By

---

Joel Altman '10

---

Daniel Herzberg '10

---

Samuel Corner '10

---

Nicholas Wheeler '10

---

Prof. David J. Olinger, advisor

---

Greg Noetscher, NSRDEC

---

Date

*Certain materials are included under the fair use exemption of the U.S. Copyright Law and have been prepared according to the fair use guidelines and are restricted from further use.*

## 1 Abstract

Currently, when deploying guided parachutes, an educated forecast for wind velocity is input into the guidance software before it is deployed, and is corrected using GPS data. Since wind velocity is variable during parachute descent, real time wind velocity data would markedly improve the parachute's landing accuracy. To solve this problem, the team designed a mechanical folding arm to extend a sensor package into the free-stream wind in order to accurately measure the wind velocity in real time and transmit the data to the parachute's guidance unit. A finite element analysis simulation study using SolidWorks Flow Simulation was conducted to determine the flow field around a parachute payload in order to properly size the length of the mechanical folding arm. The wind sensor package was comprised of five Kiel probes – a shrouded variation of standard pitot probes – arranged orthogonally so as to determine windspeed in the three Cartesian directions. The folding mechanical arm was powered by hydraulic pressure. When an internal hose is pressurized, the arm extends, and when the hose is depressurized, the arm retracts, with the help of springs. Testing of the sensor package yielded a series of equations which can be used to determine windspeed component data from the raw pressure readings of the sensors.

## 2 Acknowledgements

There are many individuals whose contributions to this project were essential to its successful completion. Specifically, the team would like to thank Greg Noetscher of NSRDEC, whose guidance and knowledge were of tremendous importance to this project. The team would also like to thank Neil Whitehouse of Higgins Shops at Worcester Polytechnic Institute and Steve Beaudet of SolidWorks Corporation for assisting in the design and fabrication of vital components of the project. Additionally, thanks are extended to Professor Eben Cobb, for his insightful input and consultation of the design aspects of the project. Finally, we would like to extend our gratitude to our project advisor, Professor David Olinger. His supervision and guidance kept us on course throughout the entirety of this project. Without the input and direction of all of these participants, the project would not have been possible.

# Table of Contents

1	Abstract .....	ii
2	Acknowledgements .....	iii
3	Table of Figures .....	vi
4	Table of Tables.....	ix
5	Introduction and Background .....	1
5.1	Project Objectives.....	1
5.2	US Military Precision Airdrop .....	3
5.2.1	Precision Airdrop Systems .....	3
5.2.2	Wind Information and Forecasting.....	5
5.3	Windspeed Sensing .....	6
5.3.1	Anemometry.....	6
5.3.2	Pitot Probes .....	7
6	Design Process.....	9
6.1	Alternative Design Concepts - Structural .....	9
6.2	Alternative Design Concepts - Sensors.....	13
6.2.1	Pressure Transducers .....	15
7	Final Design and Construction.....	17
7.1	Final Design.....	17
7.2	Computational Fluid Dynamics Simulations.....	18
7.3	Extension Mechanism.....	25
7.4	Sensor Package .....	28
7.5	Test Stand .....	30
7.6	Wind Tunnel Port Cover .....	31
7.7	Mounting Rig .....	32

8	Testing .....	34
8.1	Wind Tunnel .....	34
8.1.1	Single Kiel Probe .....	34
8.1.2	Full Sensor Package Testing.....	35
8.2	STINGER Deployment Testing.....	37
9	Future Work .....	40
10	Conclusions.....	42
11	Works Cited .....	44
	Appendix A - CFD Simulation Data and Results.....	47
	A.i Requirement.....	47
	A.ii Assumptions .....	47
	A.iii Measurement Locations.....	47
	A.iv Data Interpretation.....	49
	A.v Data.....	49
	A.vi Results.....	59
	Appendix B - STINGER Arm Construction Photo Journal.....	64
	Appendix C - Single Probe Test Data .....	68
	Appendix D - Full Sensor Package Test Data.....	71
	Appendix E - Data Sheets .....	74
	E.i United Sensor Kiel Probes .....	74

### 3 Table of Figures

Figure 1 - Early rendering of the extendible arm concept.....	10
Figure 2 - Early rendering of the trailing glider concept.....	11
Figure 3 - Early rendering of drogue chute sensor package .....	12
Figure 4 - Early rendering of dangling sensor package .....	12
Figure 5 - Hot-wire anemometer diagram <sup>11</sup> .....	13
Figure 6 - Concept rendering of ducted fan sensor .....	14
Figure 7 - United Sensor 3D pitot probe, model DC .....	14
Figure 8 - EagleTree Airspeed Microsensor <sup>17</sup> .....	16
Figure 9 – The Firefly 2k system, was chosen for analysis <sup>12</sup> .....	19
Figure 10 – Analog model, with dimensions, of the Firefly 2k system, provided by NSRDEC.....	19
Figure 11 - Velocity plot from CFD analysis .....	20
Figure 12 - Top-down view of cargo flow .....	20
Figure 13 - Measurement lines in SolidWorks Flow Simulation .....	23
Figure 14 - Measurement lines for an extension mechanism mounted on the front of the cargo, facing right .....	23
Figure 15 – X-component of windspeed.....	23
Figure 16 – Y-component of windspeed .....	24
Figure 17 - Early rendering of the S.T.I.N.G.E.R. ....	26
Figure 18 - Cross-section of pressurized and extended fire hose system .....	27
Figure 19 - Depressurized, retracted STINGER, held closed by springs (with cross section) .....	27
Figure 20 - Arm section lengths (in inches) .....	28



Figure 21 - Secured longitudinal probes (cross-section) .....	29
Figure 22 - Seating sockets to keep probes aligned .....	29
Figure 23 - 3D-printed model of holding device.....	30
Figure 24 - Test stand used to secure the sensor package during wind tunnel testing. ....	31
Figure 25 - Test stand channel in the top if the Higgins Discovery Classroom wind tunnel. ....	31
Figure 26 - Custom-machined wind tunnel port for testing single Kiel probes.....	32
Figure 27 - A loaded Firefly 2k JPADS system, ready for drop <sup>13</sup> .....	33
Figure 28 - Conceptual rendering of mounting mechanism in an exploded view.....	33
Figure 29 - Test results of single probe at normal orientation to flow .....	35
Figure 30 - Test results of sensor package at normal orientation to flow .....	36
Figure 31 - Data showing consistent windspeed readings from front-facing probe.....	37
Figure 32 - Specifications of McMaster Carr extension springs. ....	38
Figure 33 - Arm construction workspace set up.....	64
Figure 34 - Alignment holes drilled before cut.....	64
Figure 35 - Alignment holes complete.....	64
Figure 36 - Cutting aluminum stock.....	64
Figure 37 - Cutting complete .....	64
Figure 38 – Rough edges.....	64
Figure 39 - Smoothing cut edges with metal file .....	65
Figure 40 - Deburring and refining edges .....	65
Figure 41 - Smoothed edges .....	65
Figure 42 - Repeat.....	65

Figure 43 - Cutting out tabs .....	65
Figure 44 - Removing tabs .....	65
Figure 45 - Tabs removed .....	66
Figure 46 - Drilling joint holes .....	66
Figure 47 – Inner joint hardware .....	66
Figure 48 - Outer joint hardware .....	66
Figure 49 - Spring attachment 1 .....	66
Figure 50 - Spring attachment 2 .....	66
Figure 51 - Completed joint (extended).....	67
Figure 52 - Completed arm assembly .....	67
Figure 53 - Test results of single probe at 30° pitch with respect to flow.....	68
Figure 54 - Test results of single probe at 60° pitch with respect to flow.....	69
Figure 55 - Test results of single probe at 90° pitch with respect to flow.....	70
Figure 56 - Test results of sensor package at 30° pitch with respect to flow.....	71
Figure 57 - Test results of sensor package at 30° yaw with respect to flow .....	72
Figure 58 - Test results of sensor package at 30° pitch and 30° yaw with respect to flow .....	73

## 4 Table of Tables

Table 1 – Dimension data for Firefly 2k system.....	19
Table 2 – Acceptable Velocity Calculations .....	21
Table 3 – Possible mounting locations for extension mechanism.....	22
Table 4 - Necessary extension distances from various faces and directions from system. ....	24
Table 5 - Test results of single probe at normal orientation to flow.....	35
Table 6- Test results of sensor package at normal orientation to flow.....	36
Table 7 - All possible locations of extension mechanism placement .....	48
Table 8 - Possible locations after removal of illogical placements.....	48
Table 9 - Final placement possibilities .....	49
Table 10 - Test results of single probe at 30° pitch with respect to flow .....	68
Table 11 - Test results of single probe at 60° pitch with respect to flow .....	69
Table 12 - Test results of single probe at 90° pitch with respect to flow .....	70
Table 13 - Test results of sensor package at 30° pitch with respect to flow .....	71
Table 14 - Test results of sensor package at 30° yaw with respect to flow.....	72
Table 15 - Test results of sensor package at 30° pitch and 30° yaw with respect to flow .....	73

## 5 Introduction and Background

In today's army, the use of aerial delivery (or airdrops using parachutes) is quite common. In Afghanistan, a combination of poor infrastructure and the threat of Improvised Explosive Devices (IEDs) make aerial delivery the safest method of delivering supplies to forces operating in remote locations.<sup>1</sup> "Reducing the landing zone size makes recovery less dangerous for ground-based military units, who often cross hazardous areas to reach supply drops."<sup>2</sup> In situations such as the one in Haiti after the 2010 earthquake, in which the main port was destroyed and the main airport immensely crowded, airdrops became an effective way of quickly delivering supplies where they were needed.<sup>3</sup> In most cases the use of round, unguided parachutes is acceptable because the available landing area is large and does not require pinpoint accuracy on part of the air drop. However, in many instances, guided parachutes are needed when the desired target area is small. Parafoils have the ability to maneuver themselves autonomously in order to land at a small, specific area. However, the weakness inherent in their guidance systems is that they do not have the ability to measure real time wind velocities, and therefore no ability to adjust for the wind's effect on the parachute's trajectory. Currently, before the aircraft takes off, expected windspeeds are measured at the base or from meteorological forecasts and uploaded to the guidance unit for the parafoil. These often-inaccurate estimates may lead a supply drop off-course in the event of unexpected wind changes.

### 5.1 Project Objectives

The Natick Soldier Research, Development, and Engineering Center's (NSRDEC) Airdrop/Aerial Delivery Directorate is tasked with "conducting research and engineering in

military parachuting and airdrop systems to: increase aircraft/airborne force survivability; improve airdrop accuracy and functional reliability; reduce personnel injuries/casualties; and lower the cost to develop, produce and maintain these complex systems.”<sup>4</sup> This division, which created the Joint Precision Airdrop System (JPADS) challenged our group to develop a real-time, on-board wind velocity acquisition system to be placed on the parachute payload. Data from this system would be transmitted to the Airborne Guidance Unit (AGU), which would use this data to make course corrections to the parachute system, thereby increasing accuracy.

NSRDEC provided the team a variety of design constraints. The main constraint was cost; the production version of our design must cost no more than one-thousand dollars. Furthermore, the system had to: 1) be no larger than a cubic foot, 2) be able to integrate with all parafoil systems in the Army’s inventory, 3) withstand the large stresses caused by the opening shock of the parafoil and the large shock cause by landing, 4) be reusable, 5) be as light as possible and 6) provide wind data from parachute launch to when the parachute was approximately ten feet above ground level, during what is known as ‘terminal maneuvers’. Additionally, the arm must retract quickly (on the order of 1-2 seconds) after terminal maneuver data is collected, to protect the sensor package from damage upon landing.

Given these constraints and objectives, the team proceeded to perform a literature search to see what experiments or research had been previously conducted. We started with JPADS, which was a study that had been performed by the Army to develop a guidance system that would be able to account for wind velocity. RoboTek and Wamore each developed a system that used a pair of CSI Wireless Vector dual-Global Positioning System (GPS) receivers in order to calculate the wind velocity.<sup>5</sup> These systems were designed for parafoils with payloads

of 2,000 lbs up to payloads of 42,000 lbs. After continuing our research, we found that the NASA had developed a sensor system for their crew reentry vehicle the X-38 called the Flush Air Data System or FADS.<sup>6</sup> FADS consists of a 9 sensor arrangement in a cruciform pattern with one in the middle, two each to left, right, top and bottom. With that arrangement, the X-38 was able to measure wind from any direction. Keeping the JPADS and X-38 in mind, we proceeded to search for any commercial system that contained a sensor system capable of fulfilling our requirements. However, due to the uniqueness of the requirements there was no commercially available system that could be used or modified for use.

## 5.2 US Military Precision Airdrop

### 5.2.1 Precision Airdrop Systems

The U.S. Army, along with the U.S. Air Force, has been developing Precision Airdrop Systems (PADS) to increase the accuracy and safety of airdrop missions.<sup>7</sup> PADS development began in 1997 in order to address the high-altitude ballistic payload accuracy problems during humanitarian aid missions in Bosnia-Herzegovina from 1993-1995. The program was accelerated in late 2001 after similar accuracy problems were observed in Afghanistan.<sup>8</sup>

The initial objective of the PADS program was to develop a portable data processing system that allowed for ground and in-flight mission planning for ballistic airdrops. The PADS system is connected to the aircraft in order to obtain real-time wind data, both from the airplane's sensors and GPS dropsondes hand-launched from the aircraft. This real-time data is combined with weather and wind forecasts to calculate an estimated release point for ballistic airdrops to ensure their accurate arrival at the drop zone.<sup>9</sup>

The operational requirements of PADS have been expanded to include autonomously guided airdrop systems, along with 802.11g wireless communication hardware. PADS was first integrated with the Precision and Extended Glide Airdrop System (PEGASYS), a guided airdrop system, in order to form the U.S. Department of Defense (DOD) JPADS program. The PEGASYS system consists of a parachute canopy (usually a ram-air chute), AGU, and a rigging platform. The PADS hardware and software package allows for pre-flight programming planning along with simple in-flight mission, threat, environment and terrain changes. This capability allows for an immediate reaction by the user to any deviation from the original mission plan, and can even be used to program flight paths around obstacles.

The current JPADS capability is for loads between 2,000 and 42,000 pounds from altitudes up to 25,000 feet mean sea level (MSL). The JPADS objective is to provide the capability to deliver payloads ranging from 200-60,000 pounds at altitudes up to 35,000 feet MSL via autonomously guided airdrop from C-130, C-17, and other aircraft to multiple ground impact points within a 50-100 meter Circular Error Probable (CEP).

The proliferation of Man Portable Air Defense Systems (MANPADS) and Improvised Explosive Devices (IEDs) presents a significant threat to both air and ground personnel on resupply missions, particularly those in hostile areas. American and Allied aircraft cannot meet accuracy standards when higher than 2000 feet above ground level (AGL), and dropping from below this threshold causes the aircraft to become a target of small arms, Anti-Aircraft Artillery (AAA), and MANPADS threats. JPADS allows aircraft to release payloads at higher altitudes than non-precision airdrop, and autonomous payloads have the in-flight capability to adjust to dynamic weather conditions. Deploying from high altitudes makes it difficult to locate the

aircraft by sight or sound, even in high visibility conditions. Due to the high glide ratio and maneuverability of ram-air parachutes, the payload can be released from any point within a relatively large area and still have the ability to guide itself to the impact point. Even if the aircraft is seen and/or heard, the observer has no way to determine the impact point of the payload. The capability of JPADS to deploy from a high altitude and potentially long standoff distance and accurately guide itself to the impact point significantly reduces the risk to both the aircrews and the ground assets by minimizing their exposure to enemy combatants.

## 5.2.2 Wind Information and Forecasting

JPADS guidance assumes the wind velocity at any point of the trajectory is known. Currently there are several methods used to obtain wind information while en route to the drop point: download forecast wind data from an external source, pilot reports from the aircraft, dropsondes released by the carrier aircraft or another aircraft, or instrumented balloons released by personnel near the desired impact point.

When a transceiver is available, the JPADS mission planner (JPADS-MP) can be linked to a secure satellite communications network in order to receive weather information. Weather information can be downloaded from the Joint Air Force Army Weather Information Network (JAAWIN), a database maintained by the US Air Force Weather Agency (AFWA). Downloaded weather forecast information typically includes a 3-dimensional cube (100x100 km<sup>2</sup> by 40-50 x10<sup>3</sup> ft) of data centered over the desired impact point.

The JPADS-MP can also interface with the carrier aircraft's communications systems to receive wind information from the pilot, GPS dropsondes, ground-based radiosondes, or other similar instrumentation. This capability allows the mission planner to supplement the



downloaded forecast data with near real-time wind information to more accurately plan the airdrop.

### 5.3 Windspeed Sensing

As the real-time wind profile deviates from the forecast profile due to natural weather fluctuations, airdrop error can be very large. This deviation increases the risk to ground personnel attempting to recover the payload during combat resupply operations. As a result, it is desirable to include sensing equipment in the guidance payload in order to incorporate real-time wind and heading information to refine the flight path of the payload. Common windspeed instrumentation includes pitot probes or some form of anemometer.

#### 5.3.1 Anemometry

Anemometers are most commonly used in static weather stations, and generally use the angular velocity of an attached bluff body (such as a windmill) to determine the velocity of the fluid flow. Design and construction of these basic anemometers is simple and inexpensive, though the moving parts decrease the durability relative to other wind sensing methods. Calibration and data analysis is also simple.

A variation on the traditional windmill anemometers is the hot wire anemometer. This type of anemometer uses a very thin electricity carrying wire exposed to ambient air. Resistance of the wire causes it to heat up above ambient temperature, and air flowing over the wire has a cooling effect. Because the resistance of most metals is dependent on temperature, a relation can be created between the resistance of the wire and the wind velocity. Hot wire anemometers can be very accurate and have a high sampling rate, though they are very delicate.

Sonic and Laser Doppler anemometers use similar concepts to measure wind velocity. Laser Doppler anemometers uses two laser beams, one that travels into particles in the air and one that remains inside the instrument. Particles flowing in the air scatter the external beam, creating a Doppler effect that is measured by a detector. This scattered light is compared to the reference beam and used to calculate the velocity of the air. Sonic anemometers use coupled transducers to measure the time it takes for sound pulses to travel the gap between them. The speed of sound will vary based on the wind velocity, allowing one to calibrate the data to obtain velocity measurements. Laser Doppler anemometers are fairly complex and expensive relative to other methods, but have excellent resolution. Sonic anemometers have no moving parts, but support struts often distort the flow, requiring wind tunnel calibration to minimize the effects.

### 5.3.2 Pitot Probes

The most basic pitot probe is a tube facing directly into the fluid flow. The tube is attached to a pressure transducer, which measures the stagnation pressure,  $p_t$ , of the fluid flow. Incorporating the static pressure,  $p_s$ , the Bernoulli equation (shown below) is used to calculate the velocity of the fluid flow.

$$V = \sqrt{\frac{2(p_t - p_s)}{\rho}}$$

Basic pitot probes are not able to account for changes in the yaw or pitch angle. If the head is not parallel to the fluid flow, errors will be present in the stagnation pressure readings. If the orientation of the probe is fixed or measured by an external sensor, correction factors can be applied to the readings. Kiel probes are a modification of the basic pitot probe, and are used to measure the stagnation pressure in fluid flow where the angle is not known or varies during

sampling. Within certain limits,  $\pm 48^\circ$  yaw angle,  $\pm 45^\circ$  pitch angle for the probes used in this project, the Kiel probe is completely insensitive to the flow direction (see Appendix E for full data sheets on United Sensor Kiel probes).<sup>10</sup>

Pitot probes have several significant advantages over other wind sensing instrumentation. Pitot probes are simple to construct, robust, inexpensive, and generally do not require calibration. These advantages, along with the Kiel probe's relative insensitivity to flow direction, led us to choose Kiel probes as our primary wind sensing instrumentation.

## 6 Design Process

### 6.1 Alternative Design Concepts - Structural

After completing our literature search and commercial products review, we brainstormed several deployment systems for four separate concepts as well as four separate sensor systems. After considering the explicit constraints, we decided that an articulated arm mounted on the cargo system utilizing an array of Kiel probes would provide the lowest cost and the highest reliability suitable for NSRDEC's purposes. The Kiel probes were selected due to their ability to obtain accurate readings even at high angles of yaw and pitch. The articulated arm was selected because it was the least complicated deployment method and was mostly mechanical in nature leading to reduced cost and improved reliability as well as easier design.

We then proceeded to construct a demonstrator suitable for proving that the concept was in fact practical and effective. The construction only used commercially available non-military specification materials. Our testing included placing individual Kiel probes, the Kiel probe array in their container, the arm and the entire system into a closed wind tunnel at approximately sixty miles per hour windspeed.

During the brainstorming phase of the project, we looked at four possible structural designs and four sensor designs. The structures were an extendable arm, a trailing glider, using the drogue chute or the parafoil itself, and having the sensors dangling from the payload. The sensor ideas were a hot-wire/hot-film anemometer, using ducted fans, using one 3-D pitot tube, or using five separate pitot tubes. After analyzing the pros and cons of each, we narrowed the choices down to one structure and one sensor.

The extendable arm concept was promising because there were many possibilities for adaptation. There would be a mounted arm on the AGU, which could be extended into the free stream and then retracted (see Figure 1). It could be used with hydraulics or pneumatics, and could be telescoping or folding, allowing for many options. One of the foreseen complications with this design choice was that the arm might be slow to extend or retract, which was not an issue for the extension as that process was not time sensitive, but retraction must occur in approximately 1/3 to 1 second since the sensor system must remain deployed until 10 feet AGL. In order to nullify this issue in the pneumatic and hydraulic systems a high pressure reservoir could be used, however, this would incur a weight and size penalty to the design since the reservoir would need to be a large tank of compressed gas or liquid.

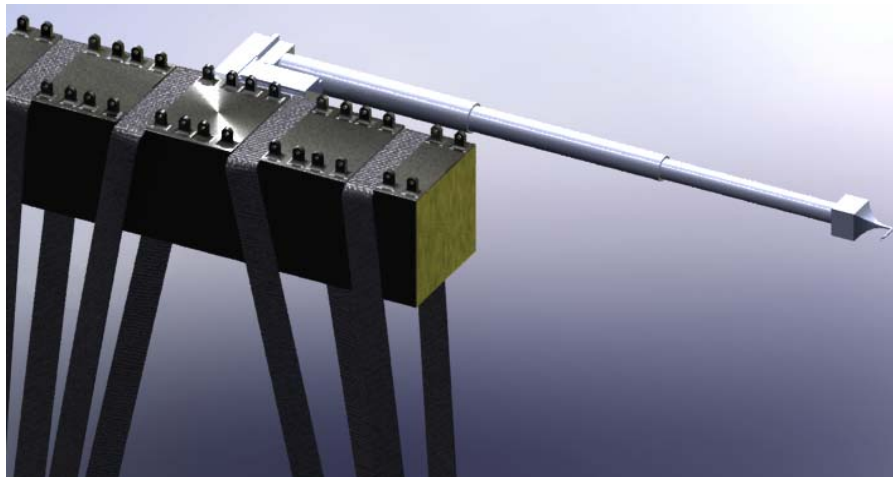


Figure 1 - Early rendering of the extendable arm concept

The second idea was to have a glider that would trail behind the parafoil system (see Figure 2). It would be attached to the AGU via a tether, and would glide behind it carrying the sensors. The benefit of this system would be that it easily avoids wake effects from the payload, it would be extendable and retractable using the tether and it would keep the sensors

from being damaged. The problem with this design was that the speed of the parachute system is so slow that a typical glider would stall, and to compensate for this, the wings would need to be much larger and this would result in greater weight and size. Furthermore, the glider would be difficult to stabilize, and any destabilization would lead to false sensor readings. Finally, the glider would need to be durable enough to survive the landing, and this too would add additional weight.

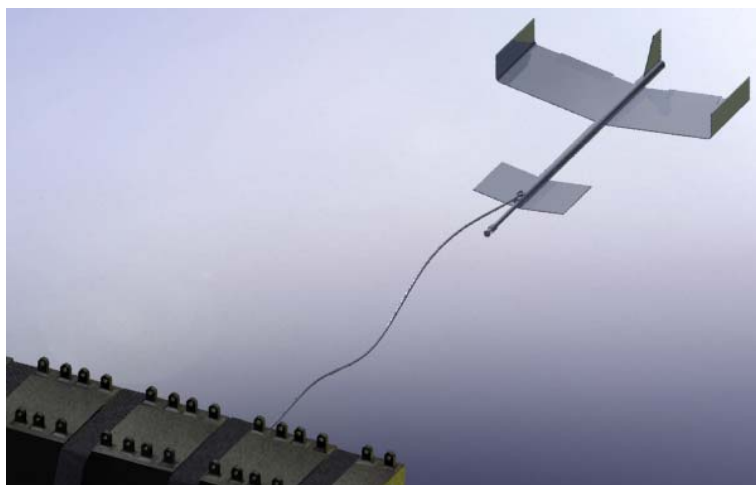


Figure 2 - Early rendering of the trailing glider concept

When the payload is released from the aircraft, a drogue chute is first deployed. The drogue chute is a small circular parachute which pulls out the main parafoil or parachute from where it is stored; however, after the deployment of the main parachute it serves no further purpose on the drop. Therefore, we thought that putting the sensor on the apex of the drogue chute would have many advantages (see Figure 3). It would be in the free stream, above any wake effects, it would be very cheap to implement, and the chute should help prevent the sensor from breaking upon landing. The problem was that the drogue chute is manufactured to

collapse once the main parachute has deployed, so drogue deployment system was quickly deemed impossible.

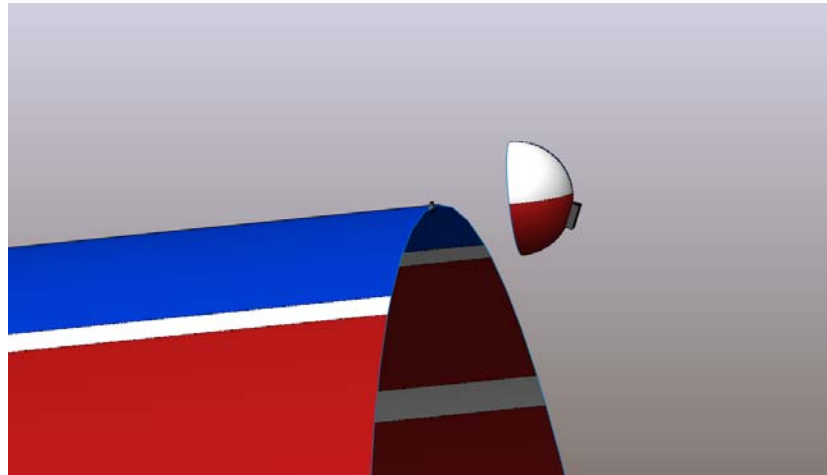


Figure 3 - Early rendering of drogue chute sensor package

The last concept for the structure was to have the sensor dangling from underneath the payload (see Figure 4). This would guarantee free stream wind, and could be retracted and extended using a winch. The problem is that no matter how it is deployed, there was no way to ensure it did not get crushed by the payload upon impact. We looked into releasing the sensor package at a calculated point prior to impact, but the likelihood of the structure and the sensors being damaged or destroyed was still very high.

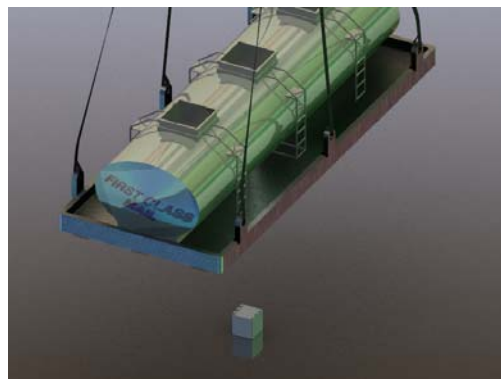


Figure 4 - Early rendering of dangling sensor package

## 6.2 Alternative Design Concepts - Sensors

For the sensor used to measure the windspeed, one of the options we explored was hot-wire/hot-film anemometers (see Figure 5). They measure resistance differences due to forced convection, and are very compact and accurate. The problem with this type of sensor is that it cannot determine the direction of the wind, which is needed for the parafoil order to compensate properly. Therefore, two sensors would be needed to measure each windspeed component. Additionally, these products were outside our price range.

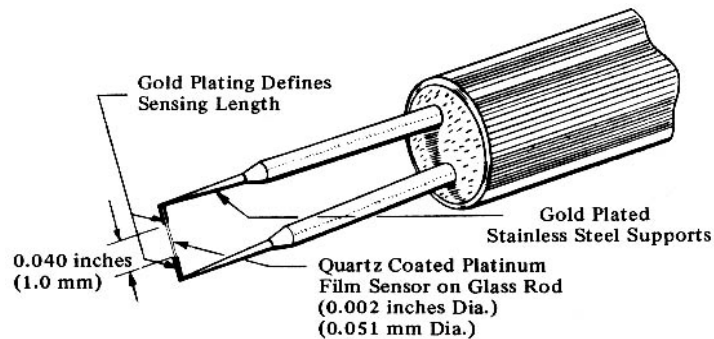


Figure 2: Cylindrical Hot Film Sensor and Support Needles- 0.002" Dia. (0.051 mm)

Figure 5 - Hot-wire anemometer diagram<sup>11</sup>

Another sensor system considered was ducted fans to measure windspeed (see Figure 6). The incoming wind spins the fan, which creates a measurable voltage that can be used to calculate the windspeed. A total of three fans would be needed, one for each direction. This arrangement would be bulky and difficult to extend into the free stream. Furthermore, additional equipment may be required to determine wind direction



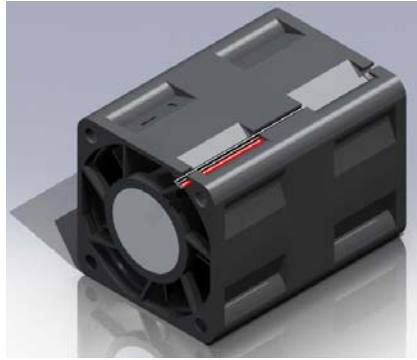


Figure 6 - Concept rendering of ducted fan sensor

The last two sensor systems use a combination of pitot probes and pressure transducers to measure the windspeed. There are three-dimensional pitot probes commercially available, which would be perfect for our applications (see Figure 7). This system is very light and small, and has the ability to separate and record windspeed in all three directions in one convenient package. However, the cost of the three-dimensional pitot probe was prohibitive. Therefore, the team considered using five different pitot tubes to accomplish the same goal (see Section 7.4). The downside is that the system must be manually assembled, and a holder would need to be specially manufactured, but the cost would be much lower and it would achieve the same end result as the three-dimensional pitot probe. One problem was that some sort of calibration would have to be determined in order to sum all of the inputs and resolve them into three Cartesian components.

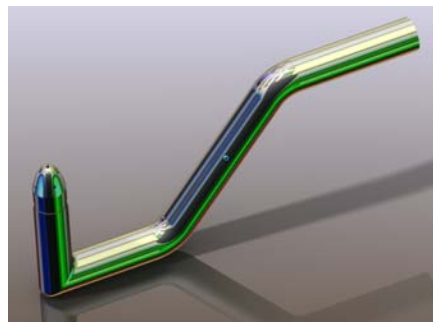


Figure 7 - United Sensor 3D pitot probe, model DC

## 6.2.1 Pressure Transducers

Use of pitot probes required the incorporation of pressure transducers in order to digitize stagnation pressure into a measurable voltage. Because the goal of this project is to measure windspeed in all three directions, it would require at least five transducers to collect accurate data. These five sensors would have to transmit windspeed values to a single transmitter, which would process the data and pass it on to the AGU. For testing purposes, we required a data logger instead of a transmitter in order to collect the voltage outputs from the sensor package. From our literature search, our team discovered that the cost of a commercially available data logger with at least five channels is nearly as much as our total budget (~\$600). Our team lacked the expertise to build our own data logger from a slightly less expensive (~\$400) component supplier.

The team decided to procure airspeed sensors from Eagle Tree Systems, who offer the Airspeed Microsensor, a compact sensor package that reads the pressure differential between a static port and a pitot probe. An image of the Airspeed Microsensor is shown in Figure 8. Though a static pressure source can be shared, each of the pitot probes used in our sensor package requires a pressure transducer. Eagle Tree Systems also offers the eLogger, a data logger and software package compatible with the Airspeed Microsensors. Unfortunately, software and hardware limitations prevent the use of more than one Airspeed Microsensor per eLogger, so a logger must be purchased for each sensor. This limitation adds significant cost to the complete sensor package, with each eLogger costing approximately \$70 and Airspeed Microsensor costing approximately \$40. For evaluation purposes, a single eLogger was purchased, along with several Airspeed Microsensors.

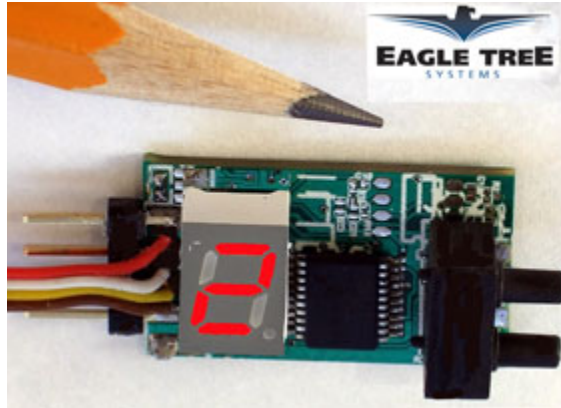


Figure 8 - EagleTree Airspeed Microsensor<sup>17</sup>

Our testing of the Eagle Tree Systems products revealed several shortcomings of the system. Our team discovered that the Airspeed Microsensors could be daisy-chained together, allowing multiple sensors to be attached to the eLogger. Unfortunately, the eLogger cannot differentiate between airspeed sensors, and instead reads all attached sensors as the same channel. This discovery means that the team would have to purchase multiple eLoggers in order to record data from the final sensor package. Additionally, wind tunnel testing showed that the Airspeed Microsensors are not accurate enough for use on this project. The sensors consistently read flow velocities at least ten feet per second slower than actual flow velocity of the tunnel. Velocity measurements from the Airspeed Microsensors were compared to measurements using the water manometer, which were comparable to the calibration curve provided with the wind tunnel. All purchased sensors read the same velocity, and communications with the Eagle Tree Systems did not produce any solution. Due to these shortcomings, the Eagle Tree sensors were not included in the final design.

## 7 Final Design and Construction

### 7.1 Final Design

After conducting research, exploring different options, and examining commercial products we finalized our design. The STINGER is a folding arm (see Section 7.3) that consists of four segments, each with different lengths such that they can fold up into a square shape; the arm segments are made out of square Aluminum tubing. At each joint, screws and washers are used to reduce the contact friction between the two segments of arm and to prevent binding on the screws themselves. Inside of the arm runs a flexible, expandable hose similar to a fire hose. This hose is inflated by a hydraulic pump and reservoir that are mounted on the base of the STINGER. When the arm needs to extend, the reservoir is emptied by the pump and the fire hose filled causing the arm to extend as the filling of the hose forces the arms to open. When the arm needs to retract, the pump reverses and the reservoir is refilled. Furthermore, at each joint is a spring that prevents the arm from opening by itself, but is weak enough such that when the fire hose is filled, the arm can open. The reason for this design is that the springs will cause the arm to retract far quicker than any other system simple system we could devise. The STINGER is mounted to the payload by means of a dual plate mechanism with one plate mounted to the base of the STINGER and the other mounted on the far side of the straps on the payload.

The sensor system is attached to the far end of the STINGER by means of a holster device that also contains the pressure transducers necessary to determine windspeed. The sensor system itself is an array of five Kiel probes mounted in a holding device which keeps them in a fixed position with one facing forward, one left, one right, one up and one down. The

Kiel probes were chosen because they do not record any windspeed beyond a certain yaw and pitch. In our case, we only want each Kiel probe to measure the wind in the direction it's facing.

## 7.2 Computational Fluid Dynamics Simulations

It was determined that in order to obtain accurate readings of the windspeed surrounding the parachute system, the airspeed sensor(s) would have to be displaced an appropriate distance from the bluff body of the cargo. To determine the distance that would provide approximately accurate results, an analog of the system was analyzed in a Computational Fluid Dynamics (CFD) program (SolidWorks Flow Simulation 2010).

With input from NSRDEC, the dimensions of an appropriate parachute system were detailed. The system analyzed was the Firefly 2k, shown in Figure 9 below. Figure 10 shows the parachute system analog developed by the MQP team in SolidWorks for fluid analysis. Note the absence of straps and other extraneous features. These components were omitted because their presence would not greatly affect the analysis results, and their behaviors cannot be properly modeled with solid geometry.



Figure 9 – The Firefly 2k system, was chosen for analysis<sup>12</sup>

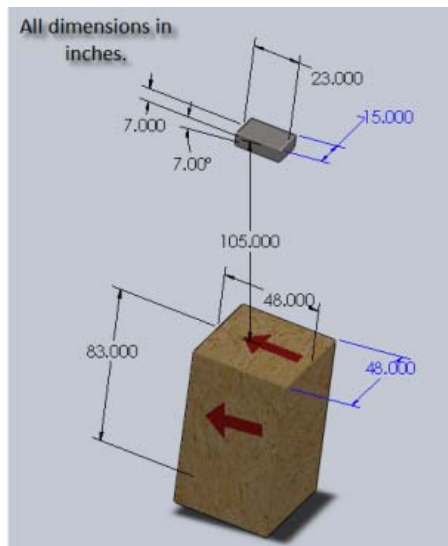


Figure 10 – Analog model, with dimensions, of the Firefly 2k system, provided by NSRDEC.

Table 1 – Dimension data for Firefly 2k system

AGU Height	AGU Width	AGU Depth	Load Height	Load Width	Load Depth	Rigging Angle	Separation
7.0 in	15.0 in	23.0 in	83.0 in	48.0 in	48.0 in	7°	105.0 in

Once the analog model was completed, it was analyzed in SolidWorks Flow Simulation. The free stream for the simulation was set to 50 ft/s in the +x-direction and 20 ft/s in the +y-direction. This data was again provided by NSRDEC as a reasonable approximation of the speed of a Firefly 2k system in flight. The air density was set to 9.3 psi, which is the density at an altitude of 12,000 ft – the Firefly’s mean altitude.

Once run, the flow simulation was post-processed and analyzed. First, images and videos were captured to further augment the team’s understanding. Selected images are shown below in Figure 11 and Figure 12.

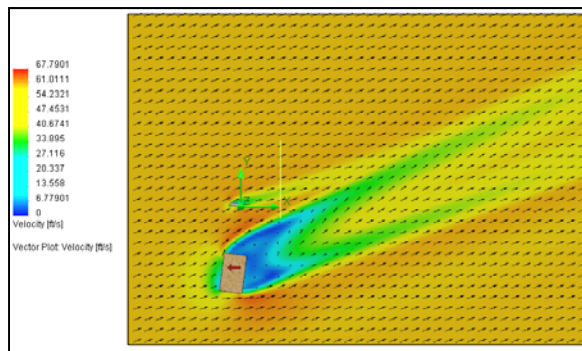


Figure 11 - Velocity plot from CFD analysis

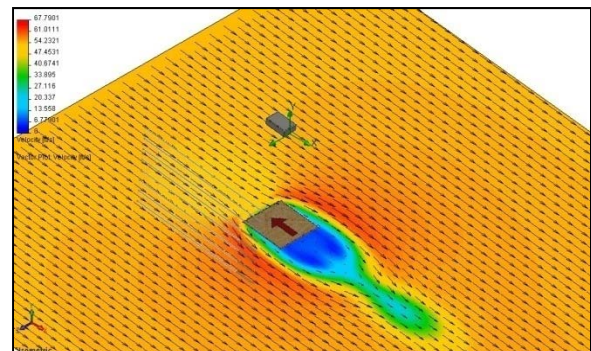


Figure 12 - Top-down view of cargo flow

Next, the data was analyzed to determine how far from the system one would have to mount the sensors to reach an approximate measurement of the free stream flow. First, an “approximate measurement” was defined to be within 5% of the prescribed free stream in any direction. Recall that the free stream was set to 50 ft/s in the x-direction, and 20 ft/s in the y-direction. Therefore, an acceptable free stream value would be one between 47.5 and 52.5 ft/s in the x-direction, and between 19 and 21 ft/s in the y-direction.

Table 2 – Acceptable Velocity Calculations

	Free Stream Value	Acceptable Error Range	Acceptable Measurement Range
X-Direction	50 ft/s	± 2.5 ft/s	47.5-52.5 ft/s
Y-Direction	20 ft/s	± 1 ft/s	19-21 ft/s

Next the team had to decide where on the system to take measurements for fluid velocity. It was physically possible to mount an extension mechanism on nearly any face of the cargo or AGU, but it may not have been practical for some locations. Below is a list of locations that were excluded from testing:

- No measurements are taken from the back side of the system, because the back side will always have more wake effects than the front side.
- No measurements are taken between the Cargo and AGU because of high wake effects and interference from straps and other system components.
- No measurements are taken in locations such that the extension mechanism would point down from the cargo unit or AGU (in case of a failed retraction, this would surely result in the destruction of the mechanism).

In addition, certain measurement locations were discarded after a simple visual inspection of the flow simulation results. In the end, only the following locations were considered for mounting an extension mechanism:



Table 3 – Possible mounting locations for extension mechanism

<b>Cargo</b>	<b>AGU</b>
Left/right side, pointing forward	Left/right side, pointing forward
Front side, pointing left/right	Front side, pointing left/right
Bottom side, pointing forward	Bottom side, pointing forward
Bottom side, pointing left/right	Bottom side, pointing left/right
Center, pointing forward	

Before measurement began, certain assumptions were made. It was first assumed that results are symmetrical for both the left and right sides. Therefore, only one set of measurements needed to be made for those locations. Second, it was assumed that the normal distance between the face on which the arm is mounted and the sensor is negligible. Therefore, measurements can be taken directly on these planes.

One of the post-processing tools available in SolidWorks Flow Simulation – called XY Plot – allows one to take measurements of nearly any property (i.e. velocity, pressure, etc) along a line drawn in space, and then plot the results of those measurements against distance. Using this tool allowed the team to determine the minimum distance from the system at which the free stream velocity reached an acceptable value, as described above.

A number of evenly spaced lines were drawn on each possible mounting point, in the appropriate direction (see Figure 13). Data on the x- and y-components of velocity were then extracted from these lines using the XY plot tool and plotted in Microsoft Excel, along with the acceptable range of free-stream measurements. An example of these results can be seen in Figure 15 and Figure 16, and the complete collection of results can be found in Appendix A.

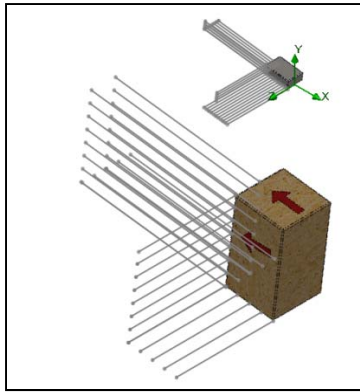


Figure 13 - Measurement lines in SolidWorks Flow Simulation

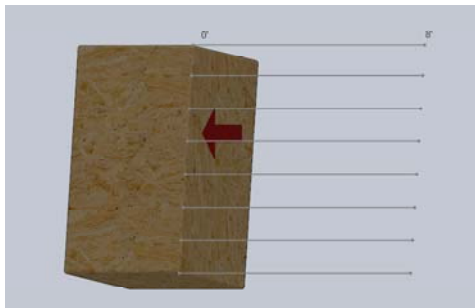


Figure 14 - Measurement lines for an extension mechanism mounted on the front of the cargo, facing right

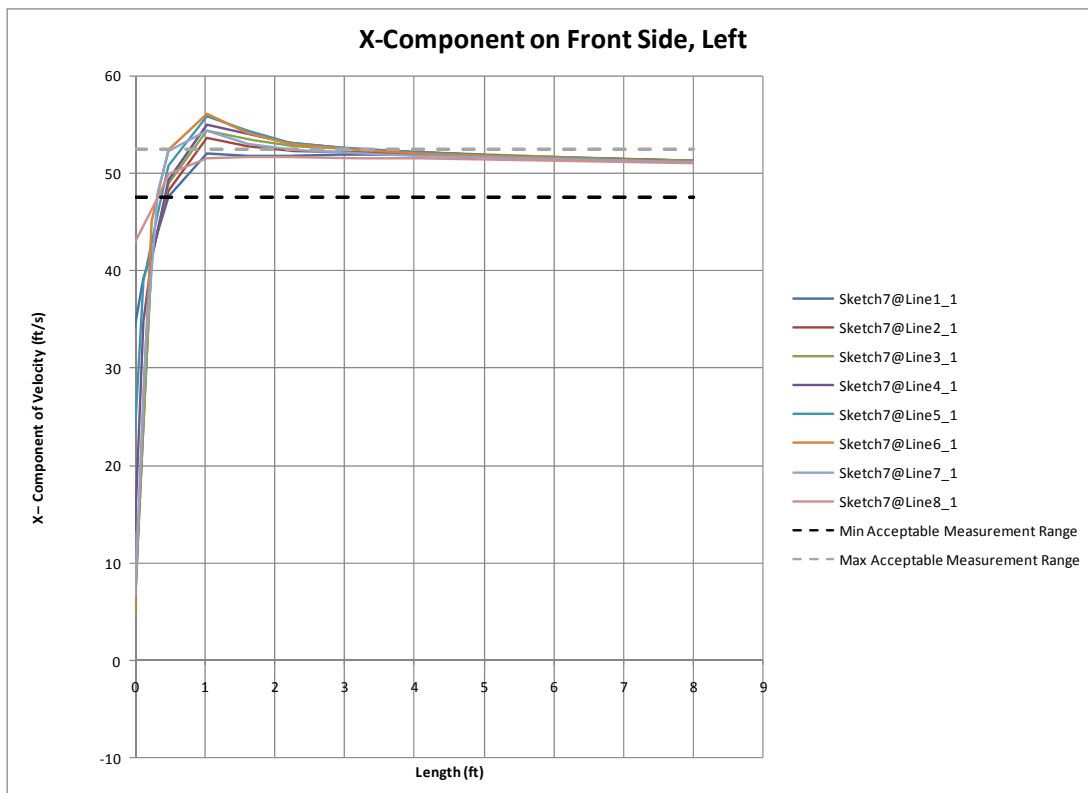


Figure 15 – X-component of windspeed

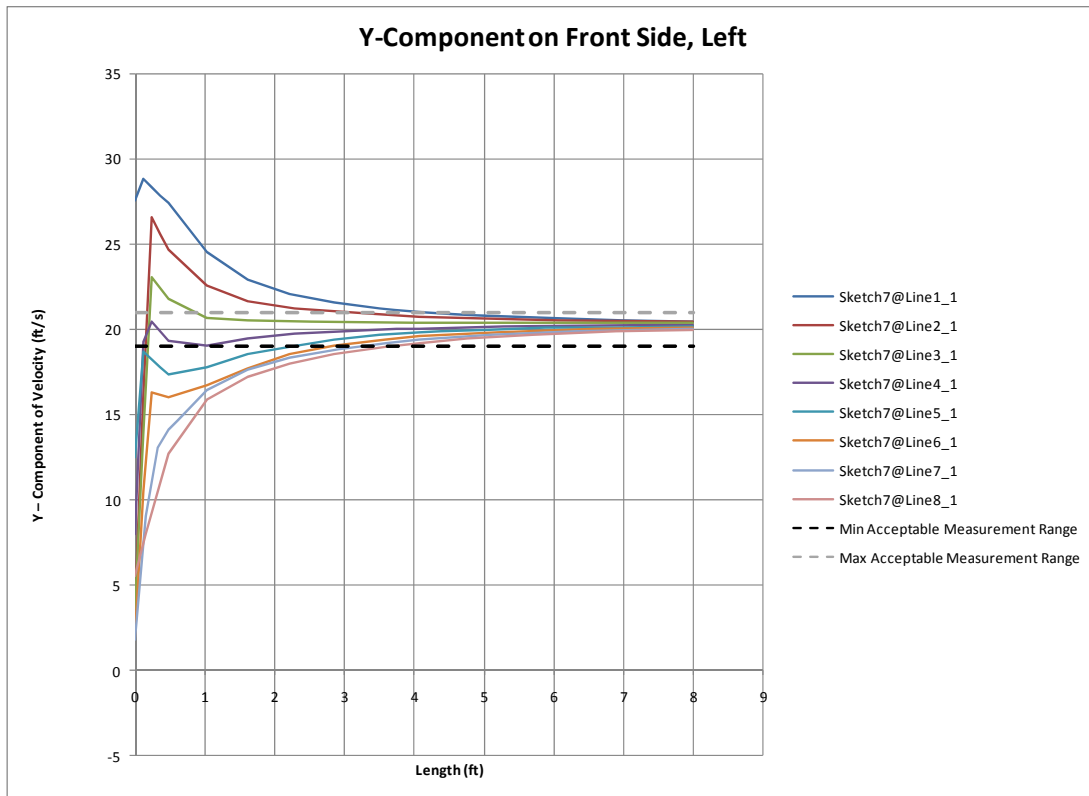


Figure 16 – Y-component of windspeed

Note that the dashed lines in the above figures represent the range in which the free stream measurement is deemed acceptable ( $\pm 5\%$ ). The solid lines represent the windspeed data taken from the sketched lines. Each color represents a different line. In interpreting the charts that were created, the results were considered acceptable only when data from all axes converge to within the acceptable limits. In this way, an extension mechanism can be placed on any point of the specified face. No additional factor of safety is introduced.

Table 4 - Necessary extension distances from various faces and directions from system.

	Left/right side, pointing forward		Front side, pointing left/right		Bottom side, pointing forward		Bottom side, pointing left/right		Center, Pointing forward	
	X-Dir	Y-Dir	X-Dir	Y-Dir	X-Dir	Y-Dir	X-Dir	Y-Dir	X-Dir	Y-Dir
<b>Cargo</b>	6.5	9.5	4	4.75	6	5.5	6	3.5	6.25	9.5
<b>AGU</b>	0.75	6.25	0.75	6	1	5.75	1	5.75	-	-

The results of the graphs were compared, (as in Table 4) and it was determined that, to minimize the necessary extension distance, an extension mechanism should be mounted on the

front side of the cargo pallet, and extend to the left or right – perpendicular to the free stream.

This mechanism would have to extend at least 4.75 feet (or 57 inches) from the system.

Note that the X-Dir and Y-Dir columns in Table 4 signify the data only when the respective component is taken into account. For example, the horizontal velocity component of airspeed reaches a reasonable approximation of the free stream less than a foot away from the AGU in most cases, but the vertical component is still unsteady many feet away. Therefore, the total velocity component is not acceptable at that point.

### 7.3 Extension Mechanism

In finalizing the design for the extension mechanism, all of the practical knowledge that the team had gained during the design process was utilized. In researching commercially-available linear actuators, we learned that many aspects of such products are unsuitable for our needs. First, most linear actuators do not telescope, meaning that the retracted length is only half of the maximum possible extension length, which itself is usually far too short to reach our free stream distance (discussed in Section 7.2). In addition, the opening and closing speeds of commercially-available linear actuators were far slower than the 1-2 seconds the team needed, and weighed much more than was feasible for the parachute system to carry.

By this point, it was becoming apparent that the team would have to design and build a specialized extension mechanism to meet the project's needs. This mechanism would have to be lightweight, and have a retracted length which was a small fraction (one-quarter to one-third) of the extended length. It would also have to quickly extend to 60 inches, and retract just as fast. Assuming that a multi-shafted telescoping actuator would be too complex to design and construct during the scope of the project, the team came up with a multi-jointed extender, which would fold into the shape of a rectangle. This extension mechanism – shown in Figure 17

– was christened the S.T.I.N.G.E.R. (short for Sensor Translating Integrated Navigation and Guidance Extender/Retractor)



Figure 17 - Early rendering of the S.T.I.N.G.E.R.

It was originally planned that the STINGER would be operated by a series of motors, possibly including gears and chains to augment the mechanical advantage of the system. However, it was soon discovered that the torques required to move the arm sections were too great for any motors which would be small and/or inexpensive enough to suit the project's constraints.

To overcome the challenges of extending the arm, the team met with Professor Eben Cobb, from the Mechanical Engineering Department at Worcester Polytechnic Institute. Through our discussions with Professor Cobb, the team arrived at a promising design idea, which was called a “flexible kinematic device” or simply the “fire hose.” In essence, this device uses hydraulic pressure to straighten a length of hose fitted inside the STINGER arm. The high pressure inside the tubing causes any bends to straighten, thereby extending the arm to its maximum length. To retract the arm, the sections will also be fitted with springs, which will force the arm closed when the hose is depressurized. Some preliminary renderings are shown in Figure 18 and Figure 19 below.

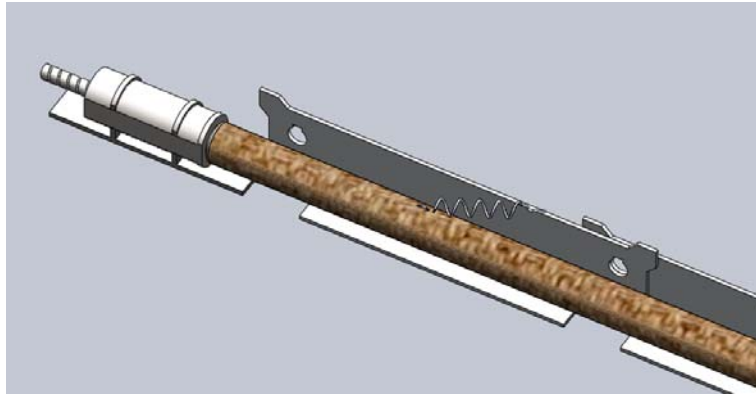


Figure 18 - Cross-section of pressurized and extended fire hose system

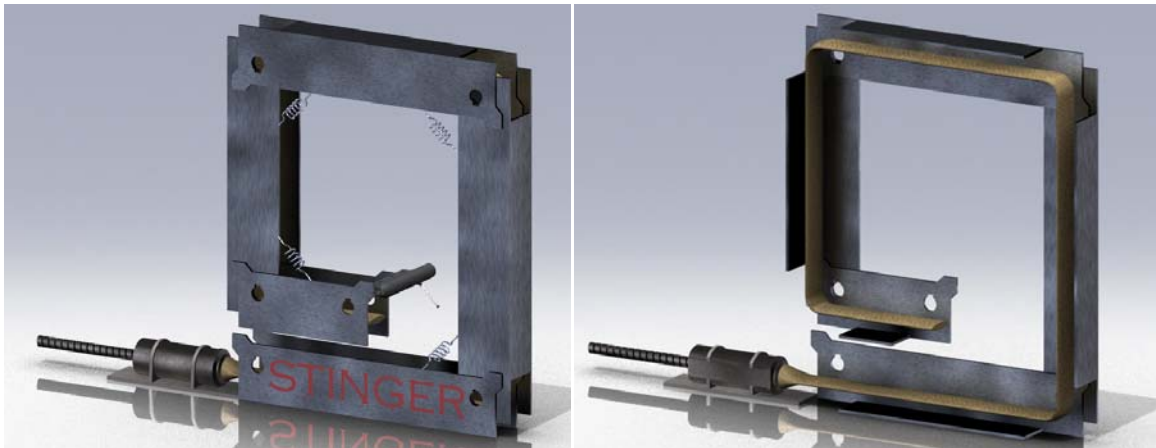


Figure 19 - Depressurized, retracted STINGER, held closed by springs (with cross section)

A high-strength, low weight aluminum (6061 Alloy) was selected for constructing the arm, to keep loading on the joints to a minimum. This material has a linear density of 0.225 lbs/ft, making it perfectly acceptable for this project. Once obtained, the aluminum stock was cut to pre-determined lengths, as illustrated in Figure 20. A full photo journal of the construction of the arm can be found in 11Appendix B. Springs, bolts, and other miscellaneous materials were also gathered, while most tools were already on-hand.

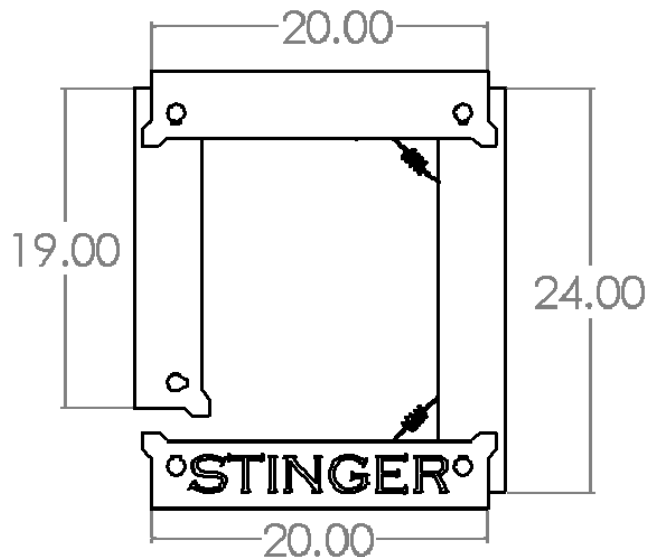


Figure 20 - Arm section lengths (in inches)

A further advantage of having multiple arm segments means that the individual arm segments can be interchanged with minimal effort. The STINGER was designed for the Firefly, but by switching arm segments the total length can be extended allowing for deployment on larger payload systems which have correspondingly larger wake envelopes. Besides the ability to increase length for use in other parafoils, individual segments allow for easy replacement and maintenance; if one of the segments has a flaw just that segment could be replaced instead of having to replace the whole system.

#### 7.4 Sensor Package

With the extension mechanism constructed, the team next needed a device which would contain the sensor package, consisting of the Kiel probes and transducers discussed above. This device would have to connect to both the STINGER mechanism, and a wind tunnel testing rig. It would also have to be relatively aerodynamic, so as not to induce any large wake effects around the sensors. Also, the device would have to securely hold the Kiel probes in their respective orientations (facing up, down, left, right, and forward) even in turbulence.

Given the dimensions of the selected Kiel probes, the holding device was designed in SolidWorks. It was designed such that four six-inch probes could fit longitudinally in the device (see Figure 21), and one probe would protrude axially from the cylinder. The seating sockets at the front of the device fit the shrouds over the tips of the probes, keeping them properly aligned (see Figure 22). A number of ribs inside the holding device provide structural stability, and also hold the probes in place at multiple points. Finally, the flanges on top will allow for simple connections to any flat plate with 3/8-inch holes. The testing rig, discussed later, was designed specifically to mate with these flanges.

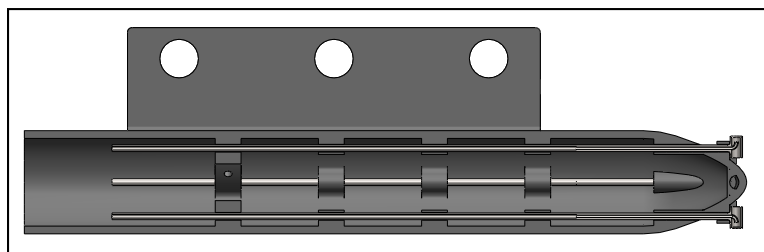


Figure 21 - Secured longitudinal probes (cross-section)

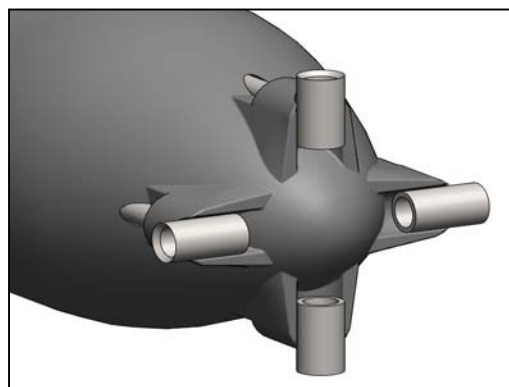


Figure 22 - Seating sockets to keep probes aligned

Once the part was designed, the team was able to quickly fabricate a prototype using a technology called 3D Printing. To begin, the SolidWorks CAD file was converted to a format called Stereo Lithography (.STL). This file format converts the model into a number of triangles comprising the positive and negative space of the part. This file was then sent to a contact at



SolidWorks Corporation, who was kind enough to offer the use of their 3D printer, free of charge. A 3D printer (in our case, a ZCorp ZPrinter 350) works by printing a single layer of these triangles at a time – at a thickness of only 0.01 inches. The positive space of the model – that which contains actual material – is printed with a gel-like acrylonitrile butadiene styrene (ABS) plastic, while the negative – or empty – space is printed with paraffin wax. Once the plastic in the finished product sets, the part is heated in a saline bath until the wax melts away, leaving only the desired part (see Figure 23). The entire manufacturing time of this part was less than 4 hours.

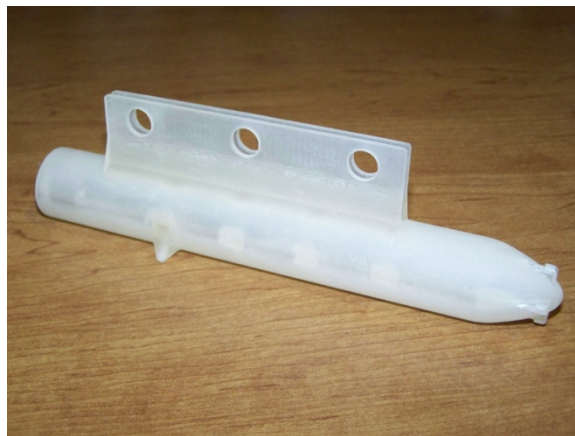


Figure 23 - 3D-printed model of holding device

## 7.5 Test Stand

Once we had completed the holding device, we needed a method of stabilizing the device in the wind tunnel so that we could test it. Thus we developed a SolidWorks model of our test stand which can be seen in Figure 24 below. With the SolidWorks model in hand, the part was machined, with assistance from Neil Whitehouse, in Higgins Labs.

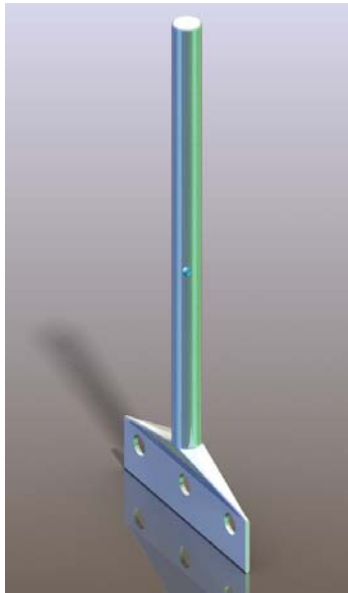


Figure 24 - Test stand used to secure the sensor package during wind tunnel testing.

As can be seen the test stand bolts into the 3/8" holes present on the sensor package holder and transitions into a steel rod. This rod passes through a narrow channel in the top of the wind tunnel (see Figure 25) and is securely fastened to the tunnel's structure.

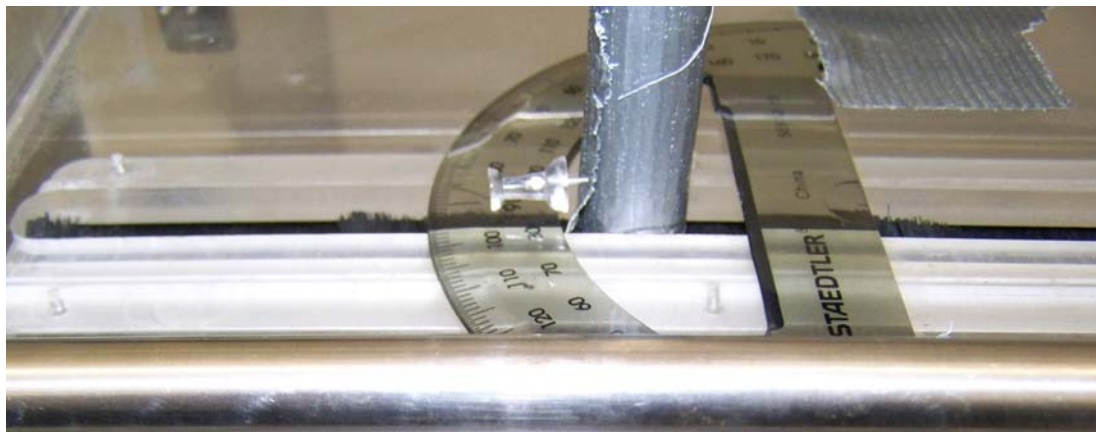


Figure 25 - Test stand channel in the top if the Higgins Discovery Classroom wind tunnel.

## 7.6 Wind Tunnel Port Cover

In addition to the test stand, we also designed a custom wind tunnel port in SolidWorks so that we would be able to securely place a single Kiel probe into the test section of the wind tunnel. Once again, Neil Whitehouse kindly machined the necessary part from a CAD model we

prepared for him. The final product may be seen in Figure 26 below. Note the small-bore hole through the center for inserting a probe.

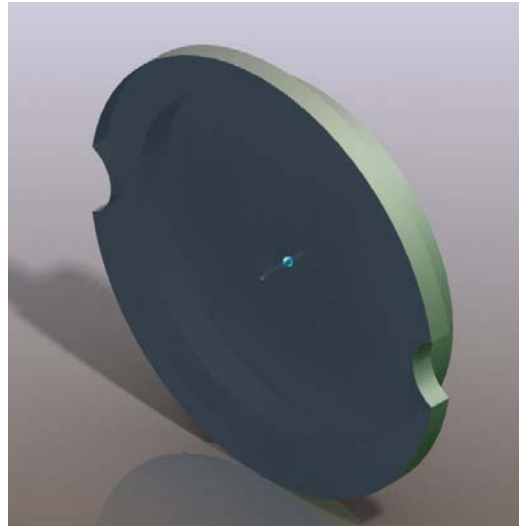


Figure 26 - Custom-machined wind tunnel port for testing single Kiel probes.

## 7.7 Mounting Rig

After developing the STINGER arm itself, the team turned its attention towards designing a mounting mechanism to connect the extension mechanism to the Firefly system. A loaded Firefly cargo pallet could come in any shape or size. Therefore, the mounting mechanism would have to be extremely versatile, with the ability to attach to nearly any shaped load. After studying the configuration of a loaded system, as seen in Figure 27, the team realized that every Firefly system will have one component in common: the straps. Using these straps as a base, the team devised an ingeniously simple method for securing the wind sensing system to the cargo pallet.



Figure 27 - A loaded Firefly 2k JPADS system, ready for drop<sup>13</sup>

The team designed a series of plates, bolted together on either side of the straps, to secure the extension mechanism in place (see Figure 28). One plate would be welded or otherwise secured to the STINGER, while the other would be inserted behind the straps of the cargo pallet. This design is extremely simple and effective since the mounting mechanism works for all payloads regardless of the size and shape.

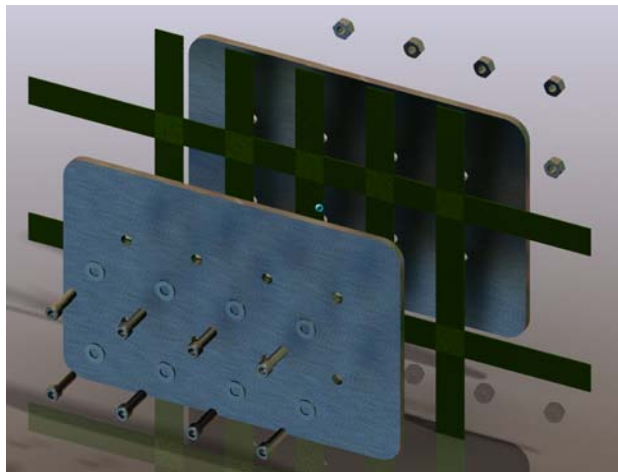


Figure 28 - Conceptual rendering of mounting mechanism in an exploded view

## 8 Testing

### 8.1 Wind Tunnel

Once the construction of the test stand, the porthole and the holding device had been completed, and the Kiel probes had arrived we needed to test our system. Single probes were tested using the Discovery Lab wind tunnel. The full sensor package could not be tested in the Discovery Lab because there was only a few centimeters clearance between the sensors and the wall when not oriented normal to the flow, which is not desirable for testing. Full sensor testing was carried out in the Higgins Fluids Laboratory wind tunnel due to its larger test section. A water manometer was used to take pressure readings.

#### 8.1.1 Single Kiel Probe

First, the team decided to individually test the Kiel probes to make sure that they were not defective in any way. We placed a single Kiel probe in the test section of the wind tunnel, using the custom designed port cover discussed in Section 7.5, and, using plastic tubing, we connected it to the water monometer. When it was connected, we varied the windspeed of the tunnel and the angle of attack of the Kiel probe, in order to determine the behavior of the probes. A sample of our test results follow, and the full set of data is available in 11Appendix C.

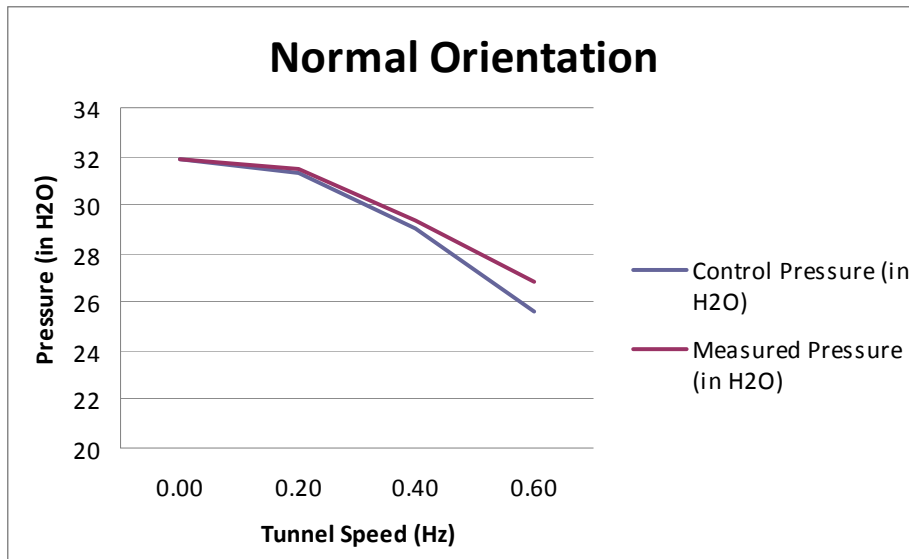


Figure 29 - Test results of single probe at normal orientation to flow

Table 5 - Test results of single probe at normal orientation to flow

Normal Orientation				
Tunnel Motor Speed (Hz)	0.00	0.20	0.40	0.60
Control Pressure (in H <sub>2</sub> O)	31.85	31.3	29	25.6
Measured Pressure (in H <sub>2</sub> O)	31.85	31.5	29.4	26.8
Difference $\Delta P$	0	-0.2	-0.4	-1.2
Calculated Windspeed	7.285831	7.245688	7	6.683313

The results of our testing with the single Kiel probes and the water monometer showed the probes were in fact giving us the correct velocity and were also not giving us any results when they were turned past their pitch limit. In the 60° and the 90° pitch experiments, some small value of velocity was recorded despite being past the pitch limit of the Kiel probe. We determined this to be a result of suction caused by high-speed flow.

### 8.1.2 Full Sensor Package Testing

Once we had ascertained that the single Kiel Probes were in fact accurate, the team proceeded to test all five Kiel probes while mounted in the holding device. The testing was conducted in the large closed-circuit wind tunnel in the Higgins Fluids Lab, which was large

enough to accommodate the full sensor package. The group tested the whole sensor system at varying speeds and orientations, similarly to the single probe tests. We tested multiple combinations of pitch and yaw at various values in order to properly test the abilities of all five Kiel probes. A sample of the resultant data is shown below, and the entirety of the test results are available in Appendix D.

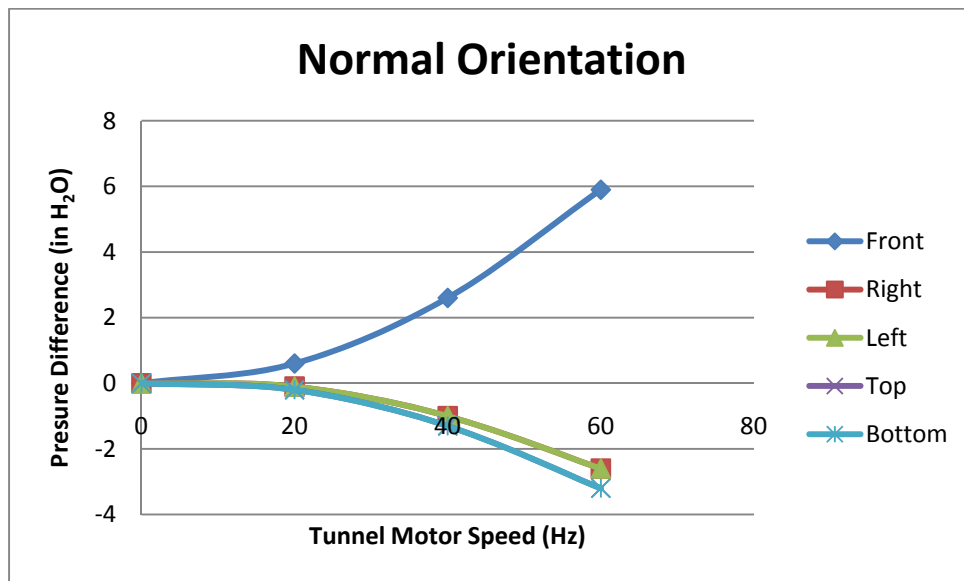


Figure 30 - Test results of sensor package at normal orientation to flow

Table 6- Test results of sensor package at normal orientation to flow

Normal Orientation								
Tunnel Motor Speed (Hz)	0		20		40		60	
	Pressure Measurement	Pressure Difference	Pressure Measurement	Pressure Difference	Pressure Measurement	Pressure Difference	Pressure Measurement	Pressure Difference
Front	31.8	0	31.2	0.6	29.2	2.6	25.9	5.9
Right	31.8	0	31.9	-0.1	32.8	-1.0	34.4	-2.6
Left	31.8	0	31.9	-0.1	32.8	-1.0	34.4	-2.6
Top	31.8	0	32	-0.2	33.1	-1.3	35	-3.2
Bottom	31.8	0	32	-0.2	33.1	-1.3	35	-3.2

The results of our testing of the entire sensor system demonstrated that our arrangement and recordings were in fact accurate; the main issue that remains for the sensor

system is to develop an algorithm that would take all of the inputs from the five Kiel probes and properly compensate for the angles involved and output the three components of the total wind velocity.

In compiling the data from our testing, the team noticed that, no matter what the speed of the wind tunnel, the front-facing probe always measured a constant speed across all orientations, to three significant figures (see Figure 31 and 11Appendix D).

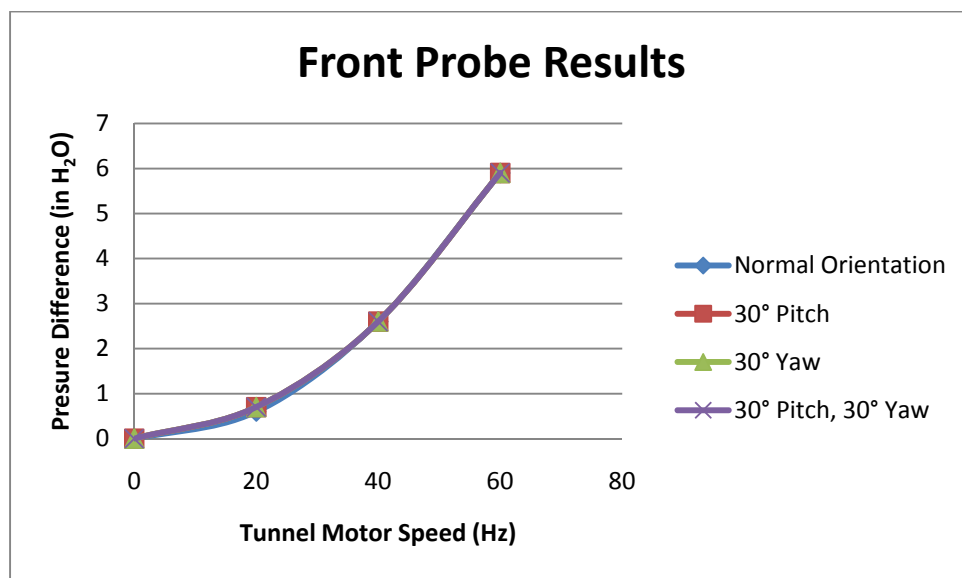


Figure 31 - Data showing consistent windspeed readings from front-facing probe

## 8.2 STINGER Deployment Testing

Once fabrication of our prototype deployment mechanism was completed, it was necessary to test its functionality to determine if it satisfies the project requirements. The project requires the arm deploy into the free stream within a reasonable amount of time ( $\approx 1$  minute) and remain rigid for the duration of the flight. Prior to landing, the arm must retract quickly (2-3 seconds maximum) in order to prevent damage during landing.



Several types springs were considered for use with arm retraction, particularly linear springs and torsion springs. After encountering difficulties attaching the torsion springs to the arm in a way that would not hinder their operation, it was decided to use linear springs for our prototype. Three springs were used, sourced from McMaster Carr, each with a spring constant of 17.75 lb/in (see full specifications in Figure 32). Once the springs were attached, the arm was manually deployed in order to test the retraction speed of the arm. After multiple tests, it was determined that the arm easily satisfies the performance requirements of the project with a very fast retraction time of 0.78 seconds. It should be noted, however that this quick and violent retraction time may cause damage to the sensor package, and should be further studied.

Extension Springs	
	
Part Number: <b>9654K334</b>	<b>\$11.39 per Pack of 3</b>
Type	Extension Springs
Material	Steel
Steel Type	Steel Music Wire
Ends	Hook Ends
Overall Length	5-29/32"
Outside Diameter	7/8"
Wire Diameter	.120"
Load	35 lbs.
Deflection at Load	1"
Rate	17.76 lbs./inch
Initial Tension	17.24 lbs.
Specifications Met	Not Rated

Figure 32 - Specifications of McMaster Carr extension springs.

Once we determined that the retraction method satisfied the project requirement, we moved to testing the extension of the deployment arm. Deployment time is not as crucial as retraction time, as there is no risk of damage to the sensor package if the arm does not deploy

quickly, though it is desirable to have a reasonably short deployment ( $\approx 30$  seconds). Due to budget and time constraints, our group was unable to locate and purchase a reservoir and pump that satisfied the project requirements (low power, low cost, low weight). In order to test the effectiveness of our hydraulic deployment method, we constructed our own piston since the water pressure of a household faucet is insufficient for our needs. Our group constructed a manual piston using a PVC pipe, a garden hose adapter, and a piston cup sourced from McMaster Carr. Reservoir volume was determined by measuring the volume of the hose used in our deployment arm, and adding a small factor of safety to account for hose deformation and compressibility. The length of the hose used in the arm is 120 inches, with an inner diameter of  $5/8$ ". Using a factor of safety of 20%, the volume of water to be used in extension is:

$$V = \left( \pi \left( \frac{d}{2} \right)^2 L \right) F = \left( \pi \left( \frac{5}{16} \right)^2 120 \right) 1.20 = 44.2 \text{ in}^3$$

## 9 Future Work

During testing and fabrication, our group noticed many areas of improvement that we were unable to act upon with the given time and budget constraints. There are several areas for improvement in all aspects of the project, and many ideas that we wished we had the time to expand on.

The primary area of improvement is in our sensing package. We found in our testing that Kiel probes may not be the correct instrumentation choice for this application. Future work should include more testing to validate our conclusion, including a new test setup for testing the full sensor package. A wind tunnel section with the ability to simulate wind gusts from a different direction than the nominal flow would be ideal for validating our sensor package. Whether this is accomplished by ducting air around to the side or some other method, it will be a challenging design project but will allow for more conclusive results on the use of Kiel probes for our application. If further testing reaffirms our conclusions about the Kiel probes, our sensor package needs to be redesigned in order to accommodate both pitot-static probes and an inertial sensor in order to provide the accurate real-time wind data needed by the guidance unit.

Another area of future work is a more in-depth look at the design of the probe shroud itself. Flow simulations should be carried out in order to determine if any of the probes in the current configuration interfere with the measurements of the rest of the sensor package. The current configuration was designed with aerodynamics in mind, but we feel this analysis should take place in order to make any necessary changes to increase the accuracy of the readings.

More work must also be done on the extension/retraction mechanism itself. Much of our time was spent trying to determine how to best deploy our sensor package to the free stream,

and we chose what we felt was the best solution. If it is decided to keep the segmented arm concept, there are many possible areas of refinement and analysis. Due to power, size, and budget constraints our group settled on using hydraulics (utilizing pressurized water) to extend the arm, and linear springs to retract it. While this approach demonstrated that the concept of using a retracting arm as a deployment method is feasible, it may be a more complex system than is necessary. In order to decrease the total size of our deployment system, research into servomotors and other hydraulic systems, or even having specialized units designed for this application should be undertaken.

Further work must also be done on the aerodynamic analysis and design of the extended arm. Though every effort was made to keep the arm as small as possible in order to produce the least amount of drag, no analysis was done on the effect of the extended arm on the flight dynamics of the cargo system. We do not want the extended arm to induce oscillations of the system, so a more streamlined shape may be required based on the results of the analysis. Also feasible would be a device that extended to the opposite side of our sensor package in order to balance out the torque created by the sensor arm.

The final area of future work would be incorporating the electronics into our sensor package. Pressure transducers are required for all the probes included on the sensor package, and an inertial sensor to determine the orientation of the sensor package is also necessary. A method of transmitting the data from our sensors to the guidance unit is needed, and the most appropriate method would be wireless transmission.

## 10 Conclusions

Our project covered a large array of options for both our extension mechanism and sensor systems. We initially started out with a massive variety of options, sixteen to be precise. We first narrowed down our sensor system choices from four down to one; we started by examining the capabilities and weaknesses of each sensor system. Two of the systems were discarded due to their fragileness and sensitive, in other words we did not feel that they were sturdy enough to withstand the landing shock and be reusable easily. One of the sensor systems was discarded because its cost was several times the budget for our entire project. The final sensor system, Kiel probes, was chosen not only by the elimination of the options but also due to its sensitivity of its yaw and pitch. With our sensor system chosen we then developed a holder device, created via 3-D printing that would secure the Kiel probes in a fixed orientation and also allow the sensors to be easily attached to our extension mechanism.

With the sensor system selected and their container constructed, we started to narrow down the possible options for our extension mechanism. We quickly eliminated some of them due to their glaring weaknesses and the difficulty involved in building them. We then selected the extending arm concept, an arm composed of multiple segments that folded upon each other in order to fulfill the size requirement. It consists of four segments that fold into a square. After multiple initial design iterations, the team eventually settled on a flexible kinematic deployment method, consisting of the small 'fire hose' inside the arm which would be filled with a hydraulic fluid, causing the hose to expand and force the arm to straighten. In order to retract the arm, the process would be reversed and the fluid withdrawn from the hose, at which point the springs positioned at each joint would contract causing the arm to retract. The springs would cause the arm to resume its initial position quickly before the impact with the

ground. The final assembled system – both in the retracted and extended position, is illustrated in Figure 33 and Figure 34, respectively.



Figure 33 - Retracted assembly: With the plunger of the test pump in the depressurized position, the springs force the arm to fold and retract.



Figure 34 - Assembly extended: with the fire hose pressurized by the test pump, the arm is forced to extend, carrying the sensor package more than five feet away from its starting position.

## 11 Works Cited

1. Rolfsen, Bruce. *Air Force Times*. January 18, 2009.  
[http://www.airforcetimes.com/news/2009/01/airforce\\_cargo\\_011609w/](http://www.airforcetimes.com/news/2009/01/airforce_cargo_011609w/) (accessed September 15, 2009).
2. National Oceanic and Atmospheric Administration. "Award-Winning Technology Improves Air-Drop Targeting." *National Oceanic and Atmospheric Administration*. September 29, 2008. [http://www.noaanews.noaa.gov/stories2008/20080929\\_airdrop.html](http://www.noaanews.noaa.gov/stories2008/20080929_airdrop.html) (accessed September 15, 2009).
3. Shaughnessy, Larry. "U.S. Air Force drops 55,000 pounds of food, water into Haiti." *CNN*. January 18, 2010.  
<http://www.cnn.com/2010/WORLD/americas/01/18/haiti.airdrop/index.html> (accessed January 21, 2010).
4. US Army Natick Soldier Research, Development & Engineering Center. *Joint Precision Airdrop System (JPADS) ACTD Team*. 2009.  
<http://nsrdec.natick.army.mil/about/airdrop/index.htm> (accessed September 7, 2009).
5. Wamore, inc. *2k Firefly*. 2009. <http://www.wamore.com/Products/Military-Products/Air-Guidance-Units-%28AGUs%29.aspx> (accessed September 2009).
6. Behr, Vance L., Dean F. Wolf, Bruce A. Rutledge, and David Hillebrandt. *Development of an 80'-Diameter Ribbon Drogue Parachute for the NASA X-38 Vehicle*. AIAA, Albuquerque, NM: American Institute of Aeronautics and Astronautics, 2001.

7. Strahan, Alan L. "Testing of Parafoil Autonomous GN&C for X-38." *17th AIAA Aerodynamic Decelerator Systems Technology Conference and Seminar*. Monterey, CA: American Institute of Aeronautics and Astronautics, 2003. 1-7.
8. Bedos, Thierry, and Brian L. Anderson. *X-38 V201 Avionics Architecture*. NASA, 1999.
9. Tavan, Steve, Greg Noetscher, Dr. Anthony Dietz, Dr. Paul Sorensen, Colin McCavitt, and Glen Bailey. "Advanced Sensors for Precision Airdrop." *20th AIAA Aerodynamic Decelerator Systems Technology Conference and Seminar*. Seattle, WA: American Institute of Aeronautics and Astronautics, 2009. 1-12.
10. Brown, Glen, and Richard Benney. "Precision Aerial Delivery Systems in a Tactical Environment." *18th AIAA Aerodynamic Decelerator Systems Technology Conference and Seminar*. Munich: American Institute of Aeronautics and Astronautics, 2005. 1-10.
11. Carter, David, Sean George, Phillip Hattis, Leena Singh, and Steve Tavan. "Autonomous Guidance, Navigation, and Control of Large Parafoils." *Draper Technology Digest* 10 (2006): 14-25.
12. Dietz, Anthony, Paul Sorensen, Ken Steele, Kristen Lafond, and Steve Tavan. "A Sodar Height Sensor for Precision Airdrops." *19th AIAA Aerodynamic Decelerator Systems Technology Conference and Seminar*. Williamsburg, VA: American Institute of Aeronautics and Astronautics, 2007. 1-10.
13. United Sensor. *Kiel Probes*. 2009. <http://www.unitedsensorcorp.com/kiel.html> (accessed 2010).
14. Payne, S.J. *Unsteady Loss in a High Pressure Turbine Stage - Chapter 4: Hot Wire Anemometry*. Ph.D. Thesis, Oxford: University of Oxford, 2001.



15. Wright, Robert, Richard Benney, and Jaclyn McHugh. "Precision Airdrop System." *18th AIAA Aerodynamic Decelerator Systems Technology Conference and Seminar*. Munich: American Institute of Aeronautics and Astronautics, 2005. 1-14.
16. Benney, Richard, Justin Barber, Joseph McGrath, Jaclyn McHugh, Greg Noetscher, and Steve Tavan. "The Joint Precision Airdrop System Advanced Concept Technology Demonstration." *18th AIAA Aerodynamic Decelerator Systems Technology Conference and Seminar*. Natick, MA: American Institute of Aeronautics and Astronautics, 2005. 1-13.
17. EagleTree Systems LLC. *Airspeed Microsensor V3*. 2005.  
<http://www.eagletreesystems.com/Standalone/standalone.htm> (accessed November 2009).

## Appendix A - CFD Simulation Data and Results

### A.i Requirement

Each separate component of velocity must be within 5% of free-stream velocity

#### X-Component

Horizontal Free Stream Value: 50 ft/s

Acceptable Error Range:  $\pm 2.5$  ft/s

Acceptable Measurement Range: 47.5-52.5 ft/s

#### Y-Component

Vertical Free Stream Value: 20 ft/s

Acceptable Error Range:  $\pm 1$  ft/s

Acceptable Measurement Range: 19-21 ft/s

### A.ii Assumptions

The normal distance between the face on which the arm is mounted and the sensor is negligible. Therefore, measurements can be taken directly on these planes. Results are symmetric for left and right sides.

### A.iii Measurement Locations

- On planes of sides of cargo container (left and right sides assumed symmetric)
- Velocity components measured on axes spaced 12" apart on Cargo, 2 1/3" apart on AGU
- Measurements around cargo are taken from 12' in front, 8' to sides
- Measurements around AGU are taken 5' (60") to all sides, An additional measurement plane passes vertically through the center of the cargo container.
- No measurements are taken from the back side of the system, because the back side will always have more wake effects than the front side.

- No measurements are taken between the Cargo and AGU because of high wake effects and interference from straps and other system components (not modeled).
- Measurements are not taken in locations such that the extension mechanism points down from the cargo unit or AGU (in case of a failed retraction, this would surely result in the destruction of the mechanism).

### All Possible Locations

Table 7 - All possible locations of extension mechanism placement

Cargo		AGU	
Left/Right, Forward	Back, Up	Left/Right, Forward	Back, Up
Left/Right, Down	Bottom, Front	Left/Right, Down	Bottom, Front
Left/Right, Back	Bottom, Back	Left/Right, Back	Bottom, Back
Left/Right, Up	Bottom, Left/Right	Left/Right, Up	Bottom, Left/Right
Front, Left/Right	Top, Front	Front, Left/Right	Top, Front
Front, Down	Top, Left/Right	Front, Down	Top, Left/Right
Front, Up	Top, Rear	Front, Up	Top, Rear
Back Left/Right	Center, Forward	Back Left/Right	Center, Forward
Back Down	Center, Rear	Back Down	Center Rear

### Existing Locations After Adherence to Above Criteria:

Table 8 - Possible locations after removal of illogical placements.

Cargo	AGU
Left/Right, Forward	Left/Right, Forward
Front, Left/Right	Left/Right, Up
Bottom, Forward	Front, Left/Right
Bottom, Left/Right	Front, Up

Top, Forward	Bottom, Front
Top, Left/Right	Bottom, Left/Right
	Top, Forward

**Remaining Locations After Visual Inspection of Flow Simulation Results:**

Table 9 - Final placement possibilities

Cargo	AGU
Left/Right, Forward	Left/Right, Forward
Front, Left/Right	Front, Left/Right
Bottom, Forward	Bottom, Front
Bottom, Left/Right	Bottom, Left/Right
Cargo Center, Forward	

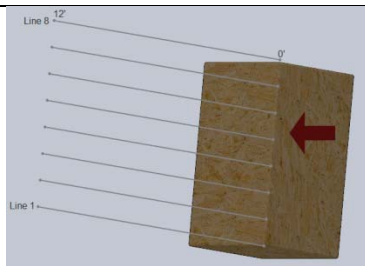
**A.iv Data Interpretation**

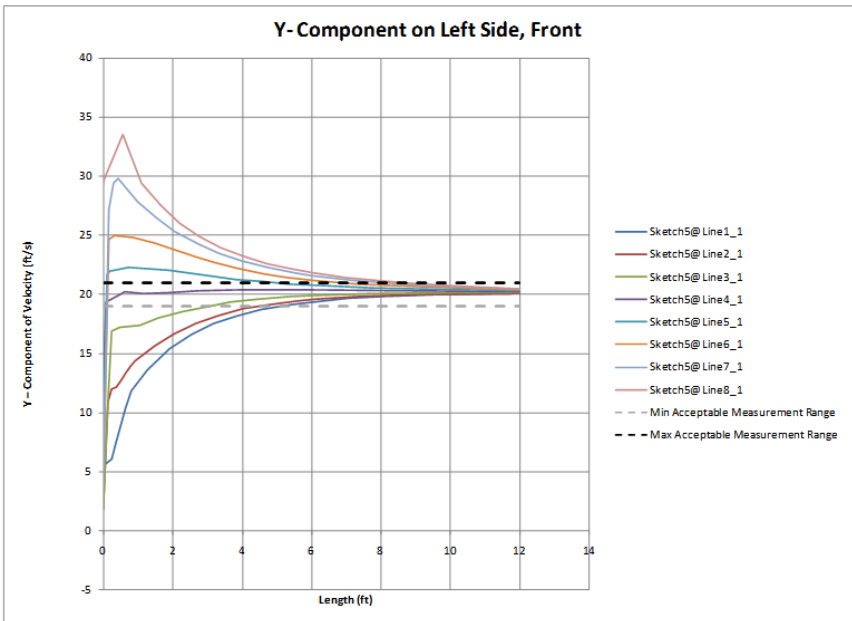
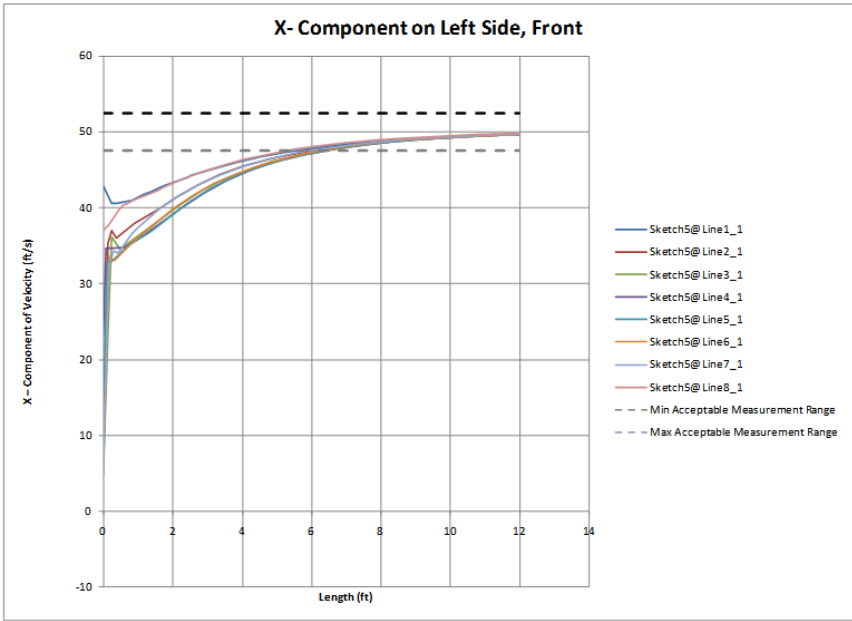
Results are considered acceptable only when data from all axes converge to within acceptable limits, described above. In this way, an extension mechanism can be placed on any point of the specified face. No additional factor of safety is introduced.

**A.v Data**

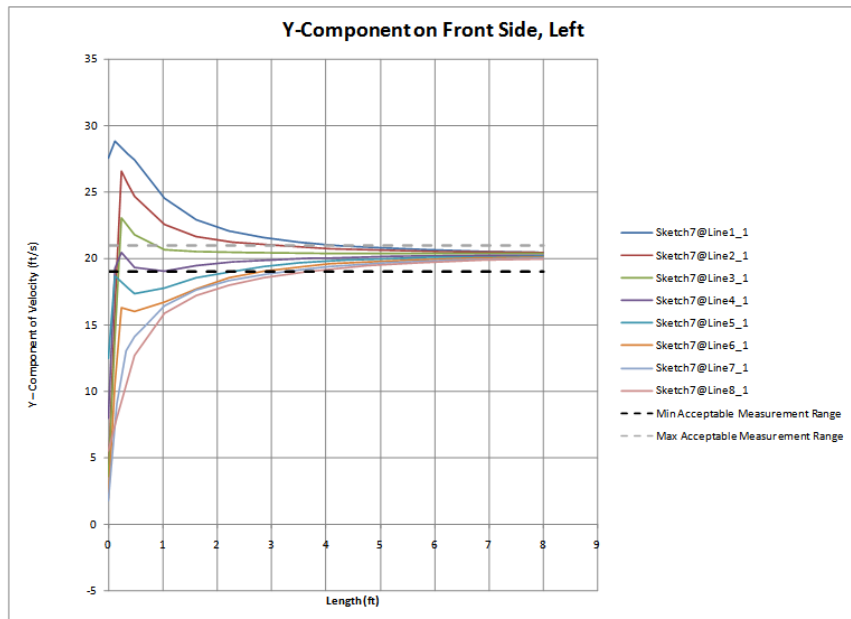
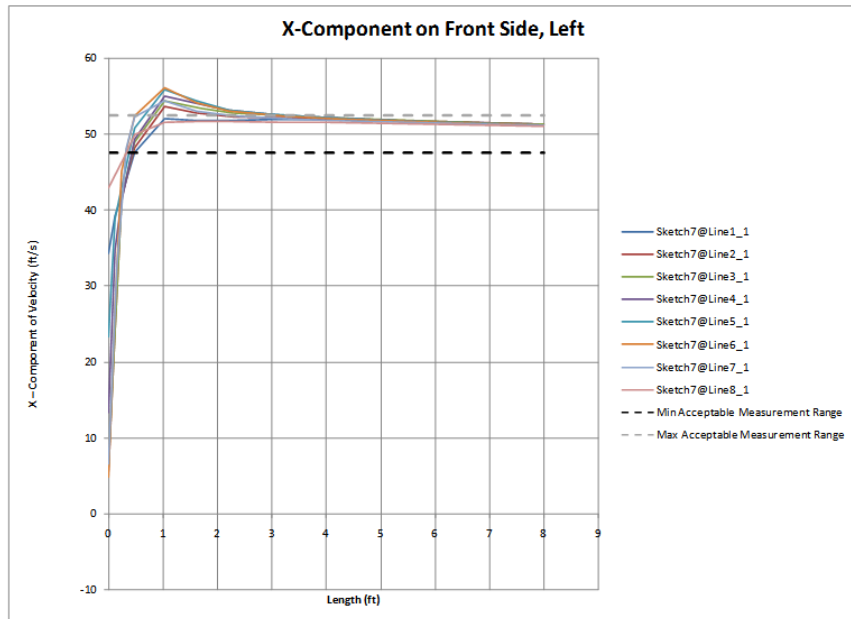
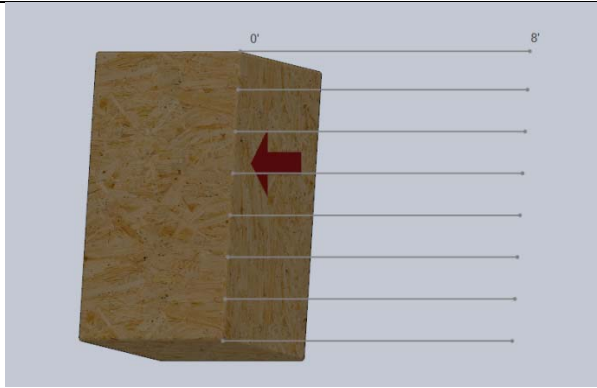
**Cargo**

**Left Side/Right Side, Facing Forward**

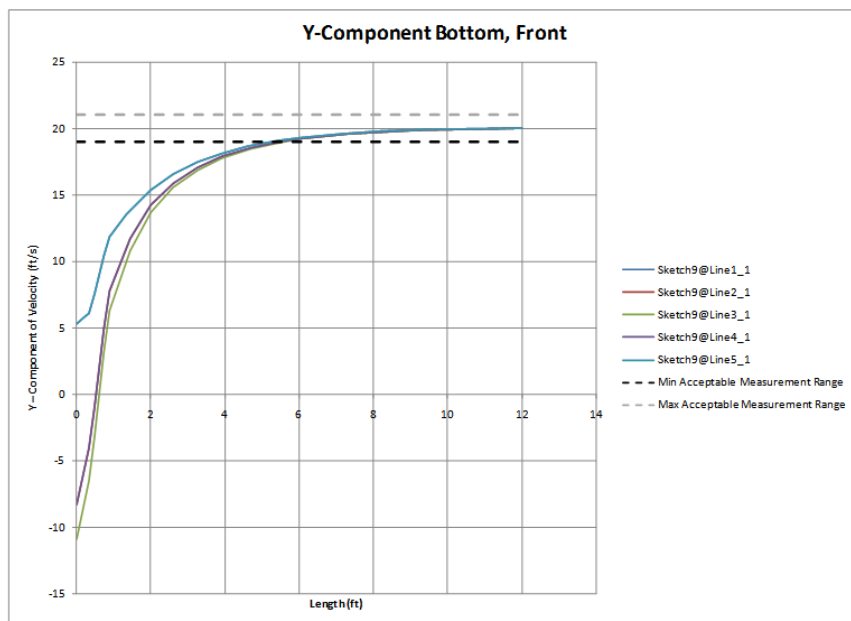
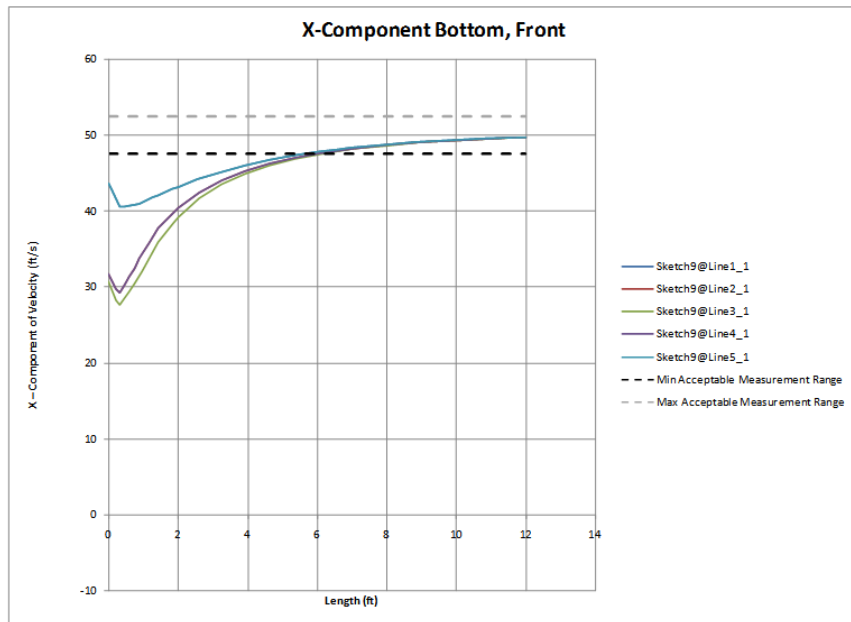
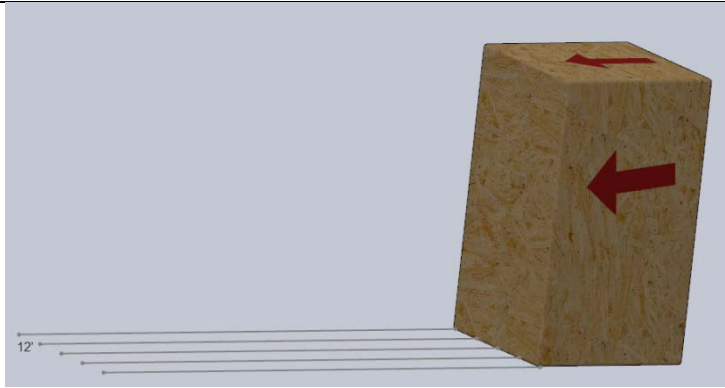




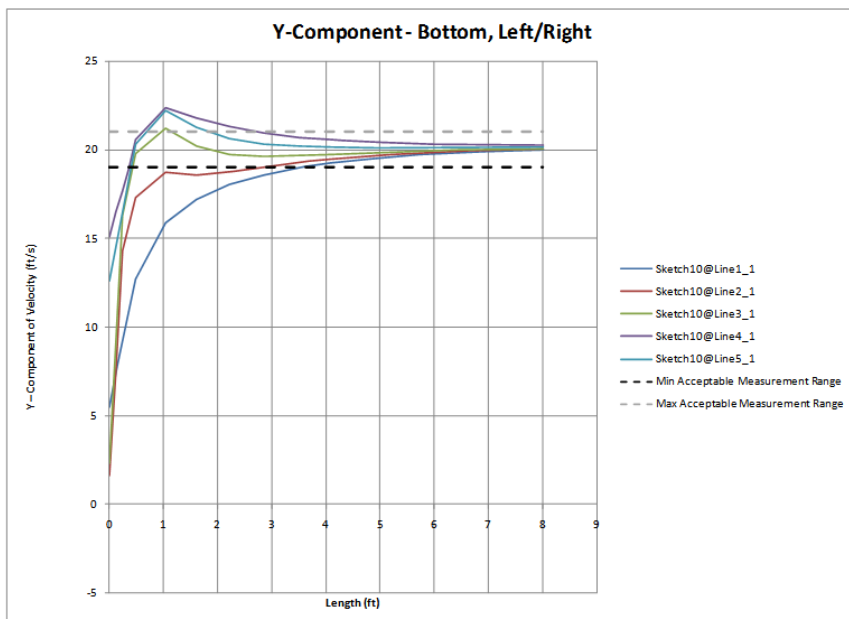
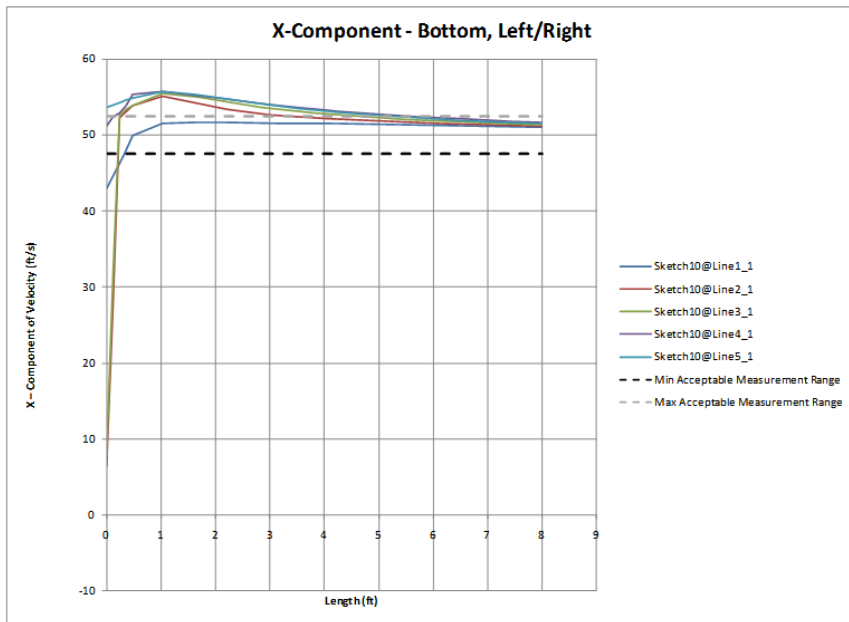
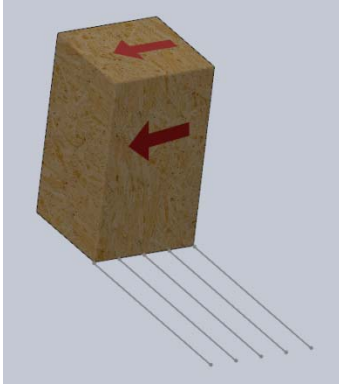
# Front Side, Facing Left/Right



## Bottom Side, Facing Front

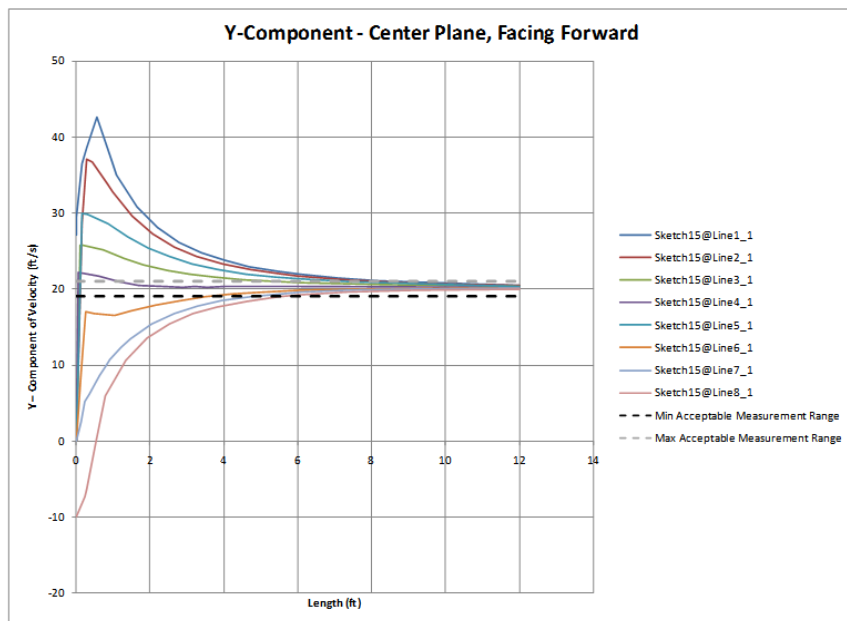
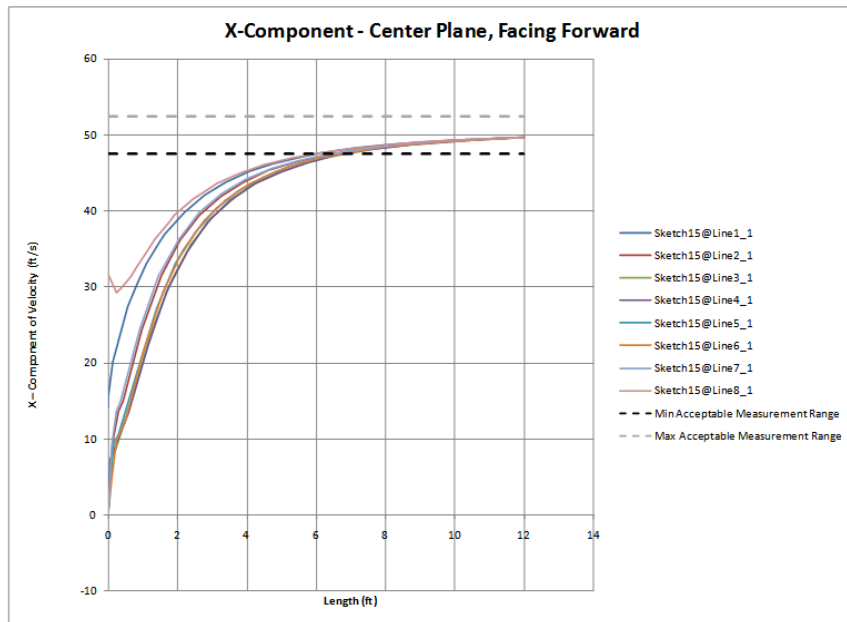
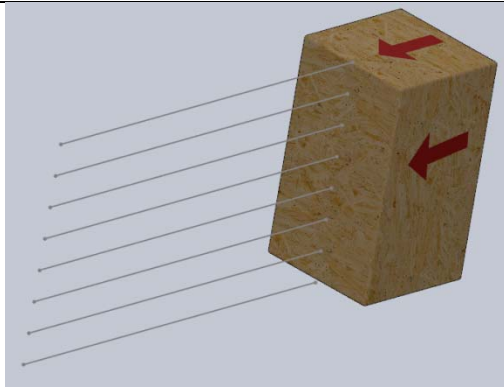


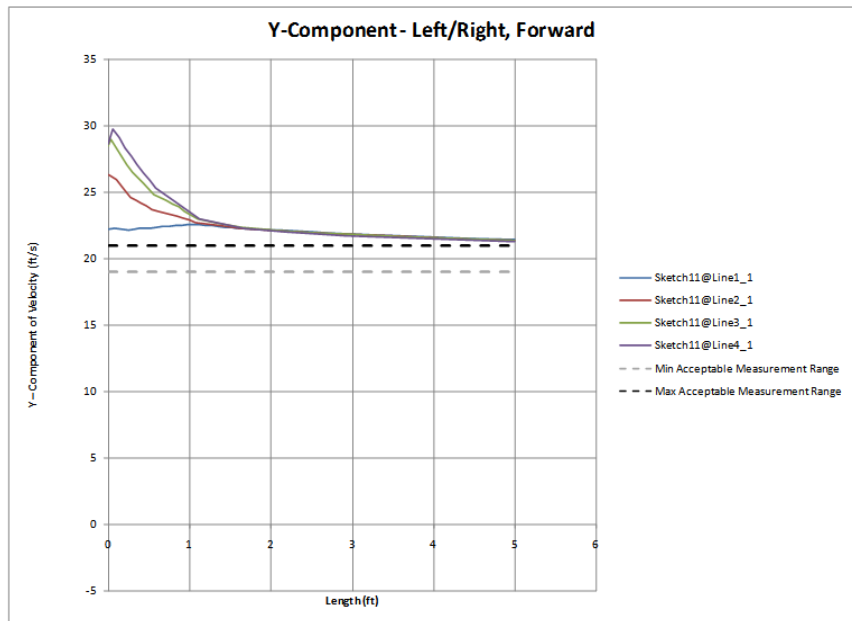
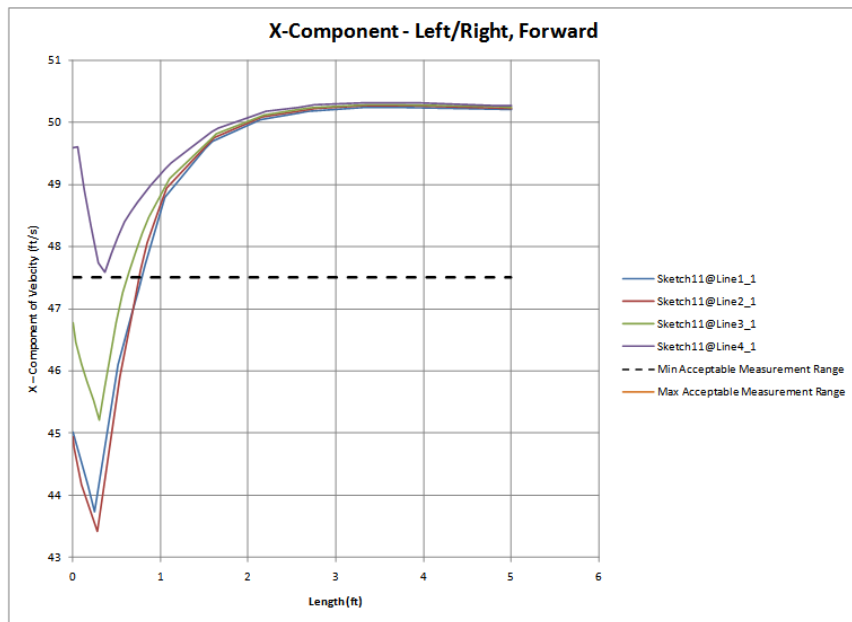
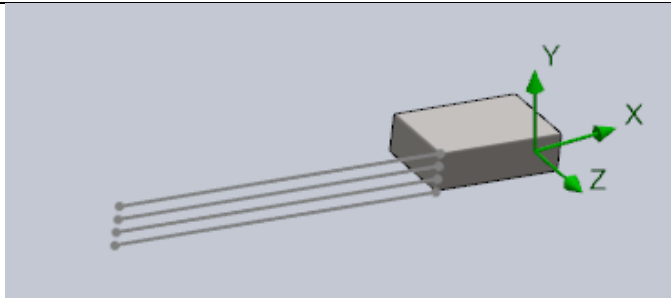
## Bottom Side, Facing Left/Right



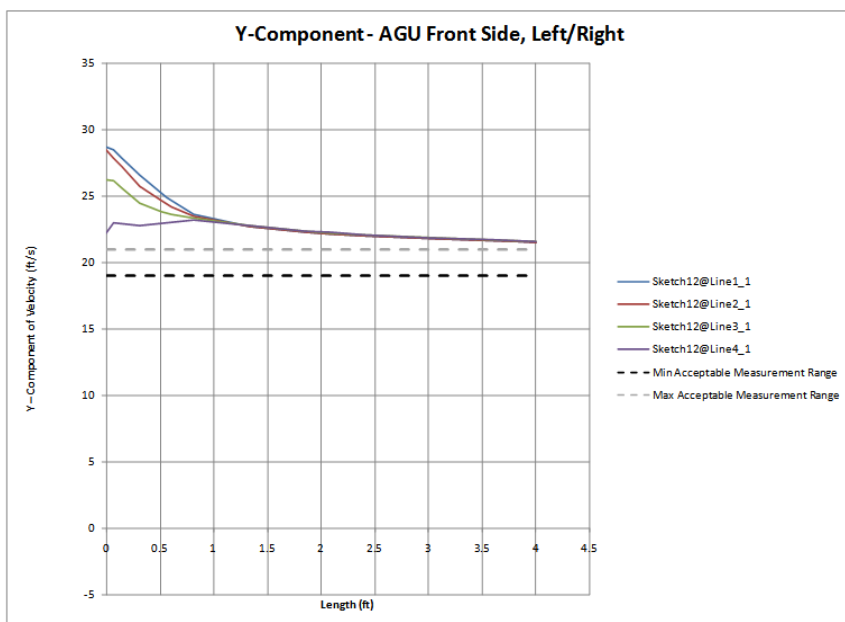
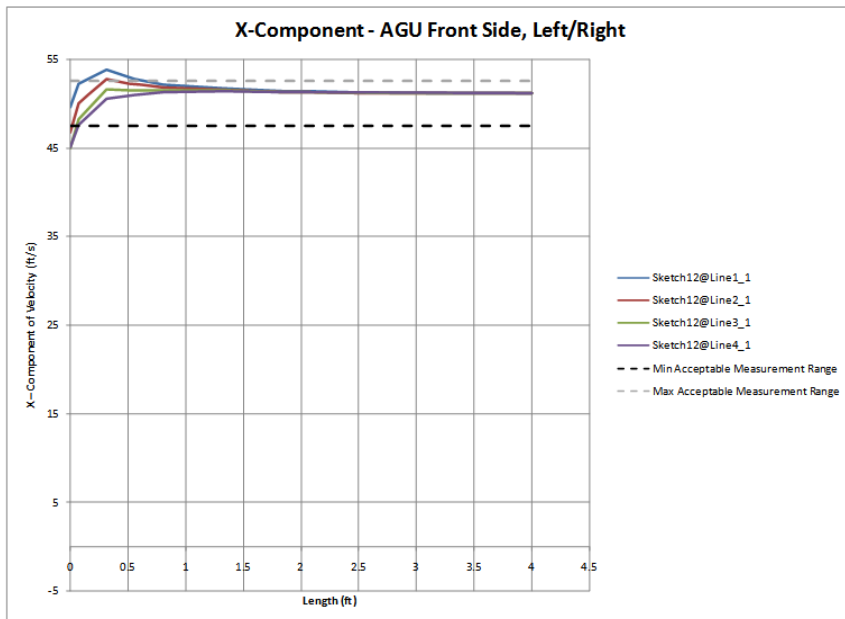
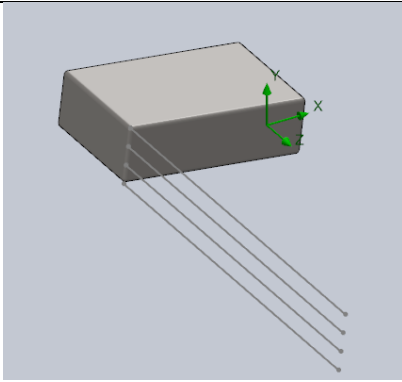


# Center, Facing Forward

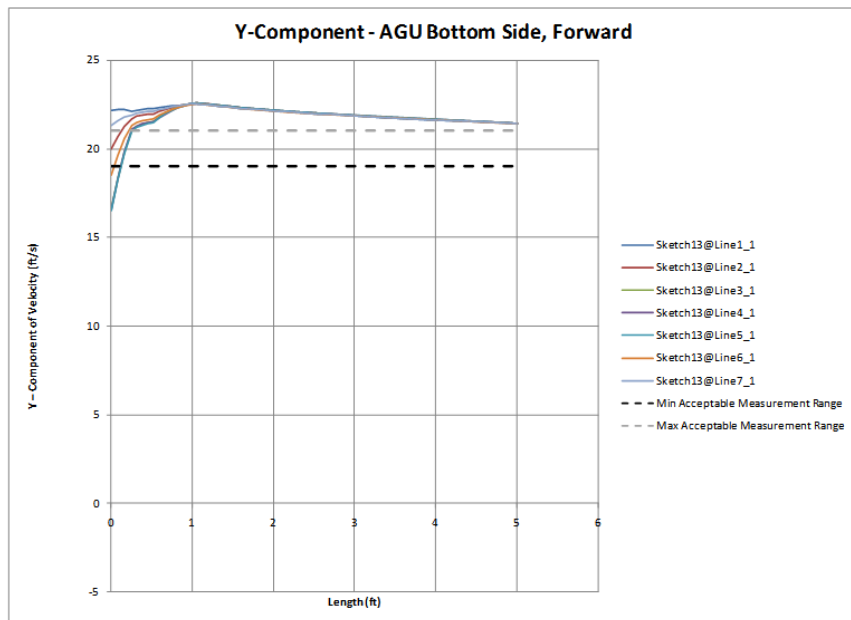
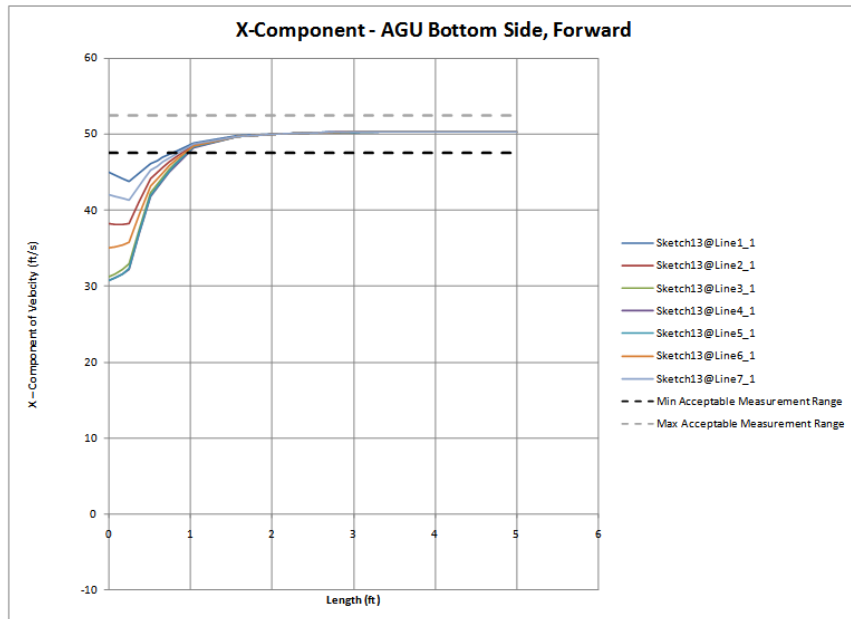
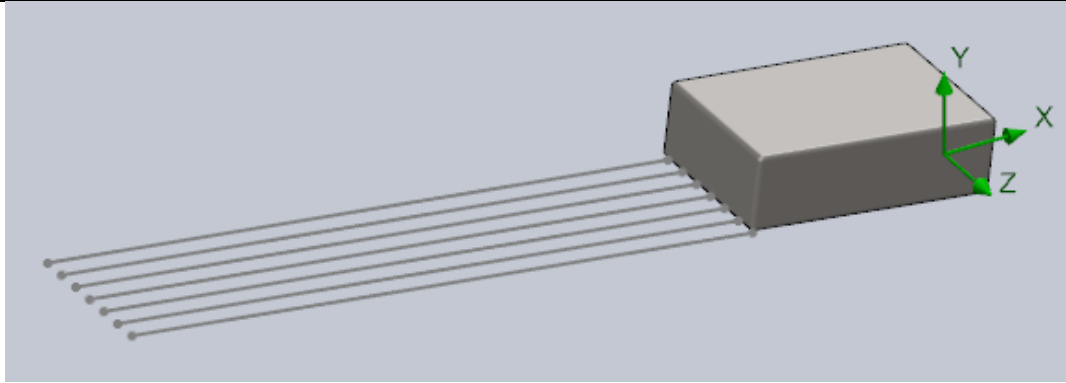




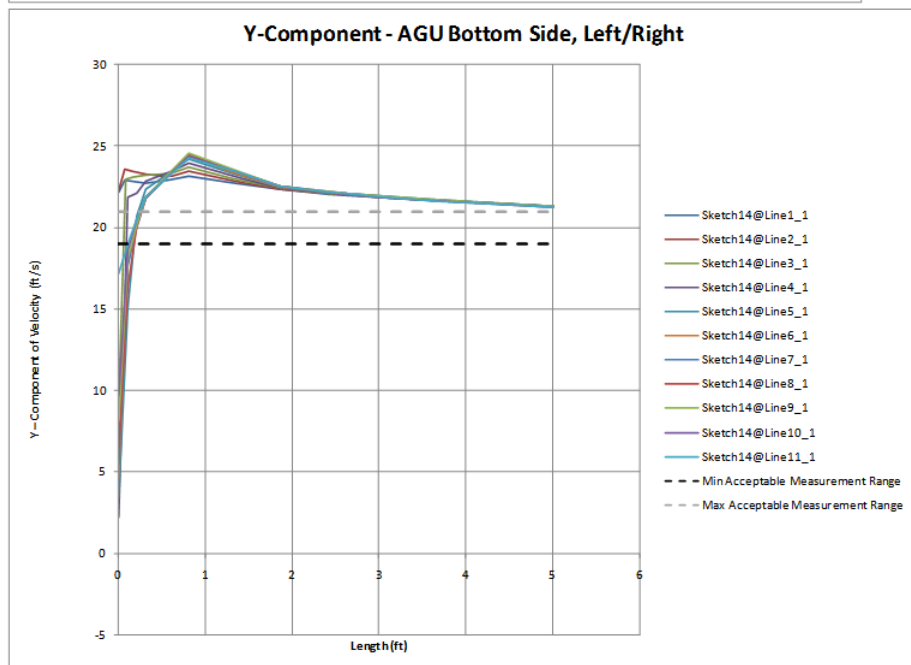
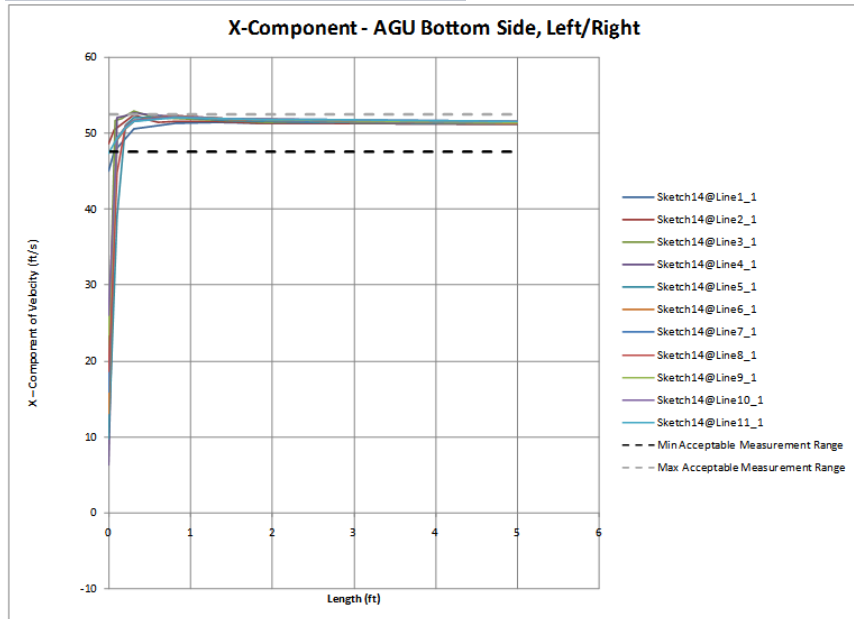
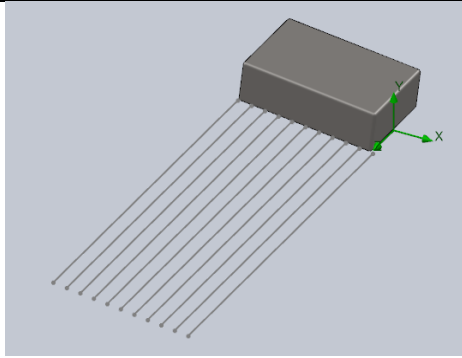
# Front Side, Facing Left/Right



# Bottom Side, Facing Front



# Bottom Side, Facing Left/Right



Cargo

Left Side/Right Side, Facing Front

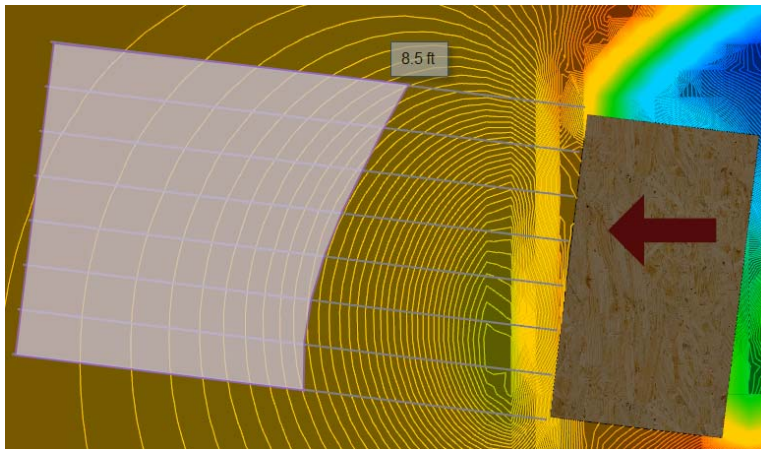
X-Component

Acceptable Extension Length: 6.75 ft

Y-Component

Acceptable Extension Length: 8.5 ft

Overall (maximum value): **8.5 ft**



Front Side, Facing Left/Right

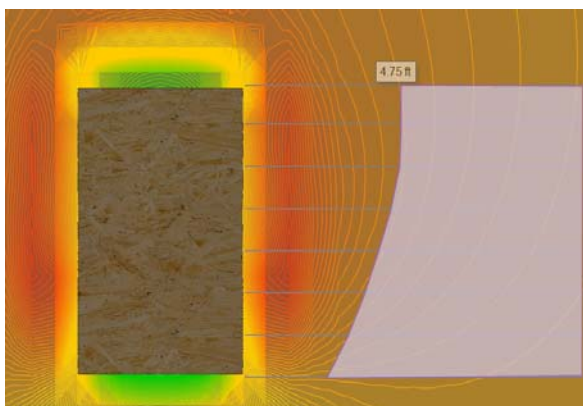
X-Component

Acceptable Extension Length: 4 ft

Y-Component

Acceptable Extension Length: 4.75 ft

Overall (maximum value): **4.75 ft**



### Bottom Side, Facing Front

---

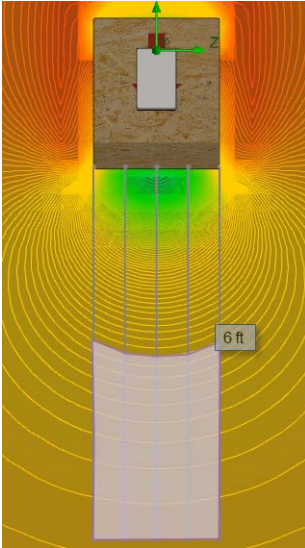
X-Component

Acceptable Extension Length: 6 ft

Y-Component

Acceptable Extension Length: 5.5 ft

Overall (maximum value): **6 ft**



### Bottom Side, Facing Left/Right

---

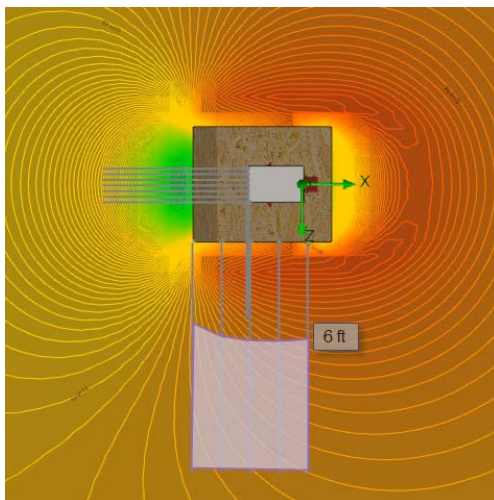
X-Component

Acceptable Extension Length: 6 ft

Y-Component

Acceptable Extension Length: 3.5 ft

Overall (maximum value): **6 ft**



## Center, Facing Forward

---

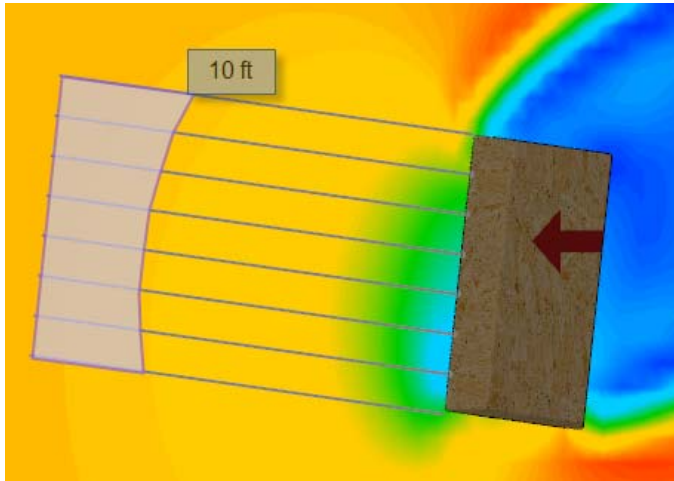
### X-Component

Acceptable Extension Length: 6.75ft

### Y-Component

Acceptable Extension Length: 10 ft

Overall (maximum value): 10 ft



## AGU

### Left Side/Right Side, Facing Forward

---

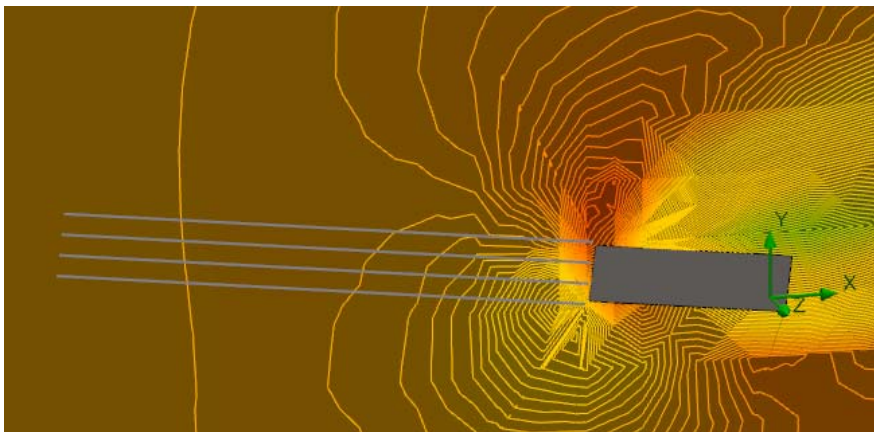
### X-Component

Acceptable Extension Length: 0.75 ft

### Y-Component

Acceptable Extension Length: > 5ft

Overall (maximum value): > 5 ft





## Front Side, Facing Left/Right

---

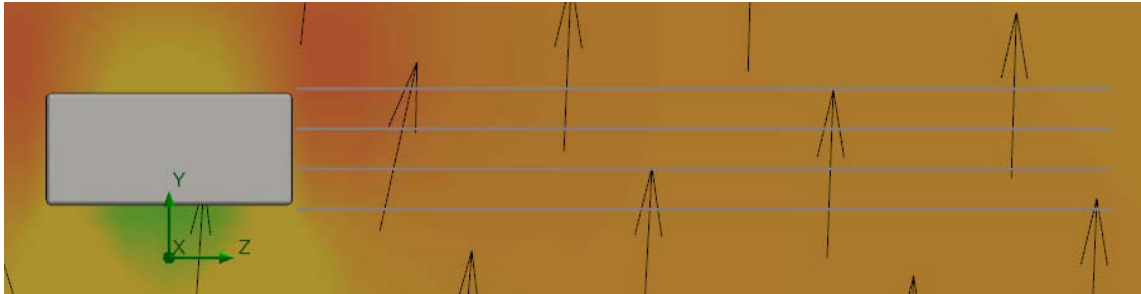
### X-Component

Acceptable Extension Length: 0.75 ft

### Y-Component

Acceptable Extension Length: > 4 ft

Overall (maximum value): > 4 ft



## Bottom Side, Facing Front

---

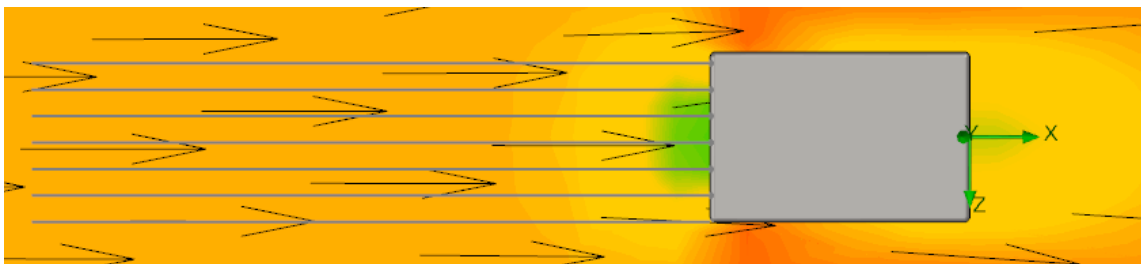
### X-Component

Acceptable Extension Length: 1 ft

### Y-Component

Acceptable Extension Length: > 5 ft

Overall (maximum value): > 5 ft



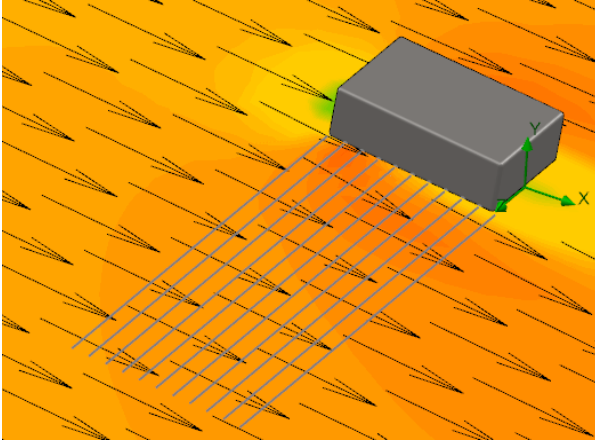
X-Component

Acceptable Extension Length: 0.75 ft

Y-Component

Acceptable Extension Length: > 5 ft

Overall (maximum value): > 5 ft



## Appendix B - STINGER Arm Construction Photo Journal



Figure 35 - Arm construction workspace set up



Figure 38 - Cutting aluminum stock

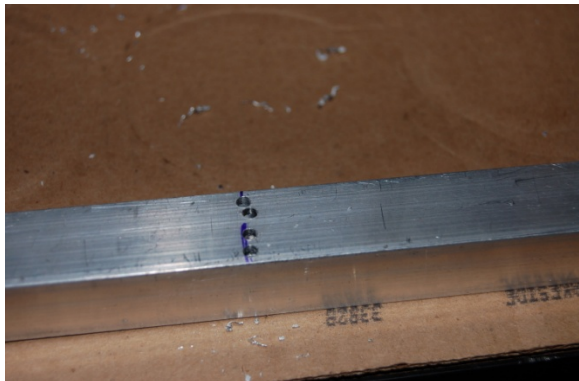


Figure 36 - Alignment holes drilled before cut



Figure 39 - Cutting complete

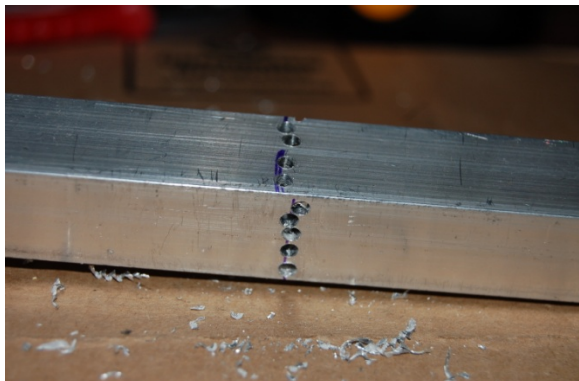


Figure 37 - Alignment holes complete

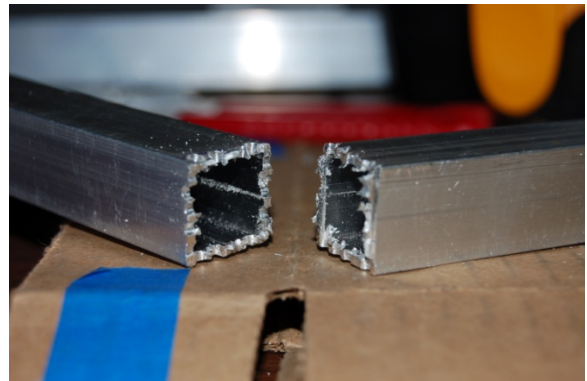


Figure 40 - Rough edges

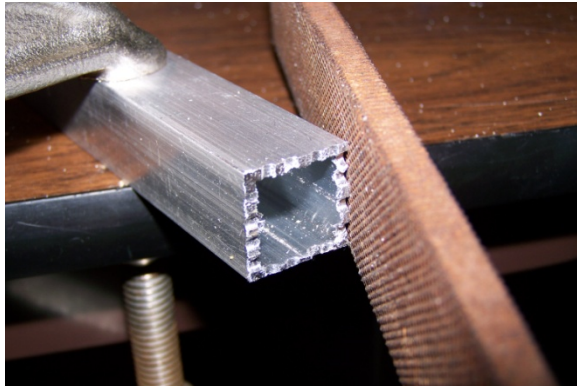


Figure 41 - Smoothing cut edges with metal file

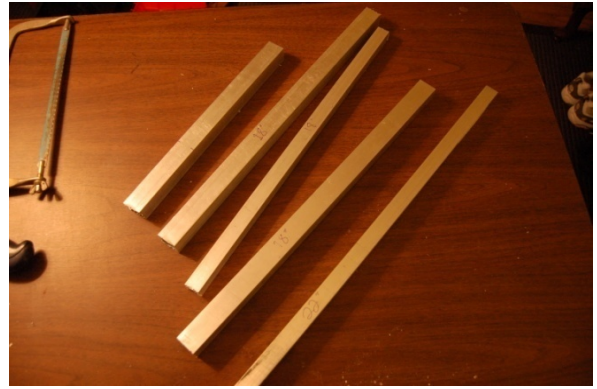


Figure 44 - Repeat...

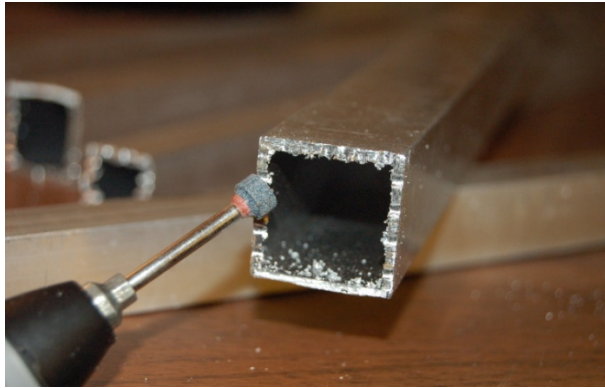


Figure 42 - Deburring and refining edges

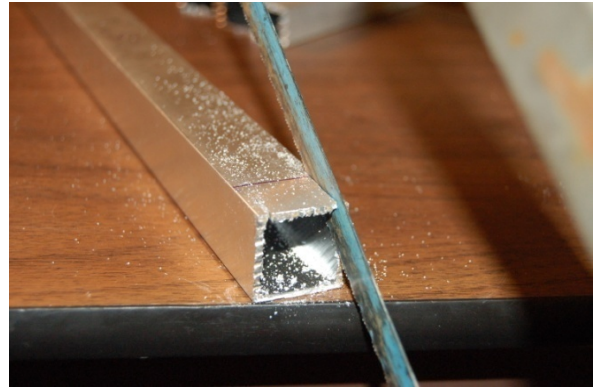


Figure 45 - Cutting out tabs



Figure 43 - Smoothed edges



Figure 46 - Removing tabs



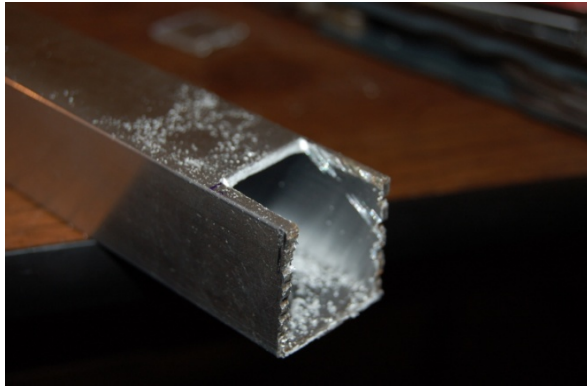


Figure 47 - Tabs removed



Figure 50 - Outer joint hardware



Figure 48 - Drilling joint holes

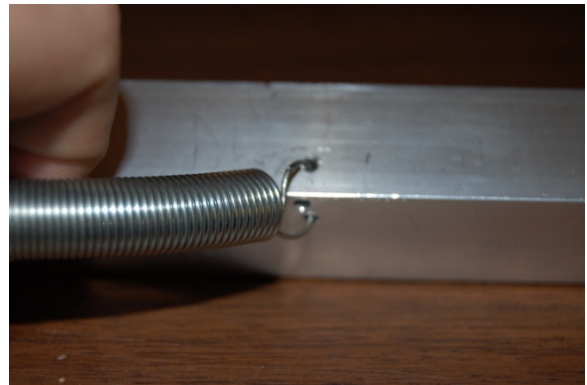


Figure 51 - Spring attachment 1



Figure 49 - Inner joint hardware

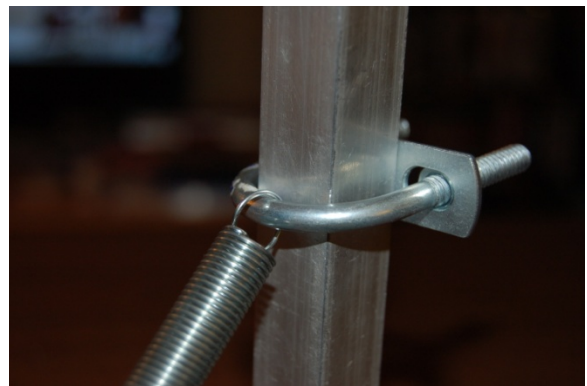


Figure 52 - Spring attachment 2

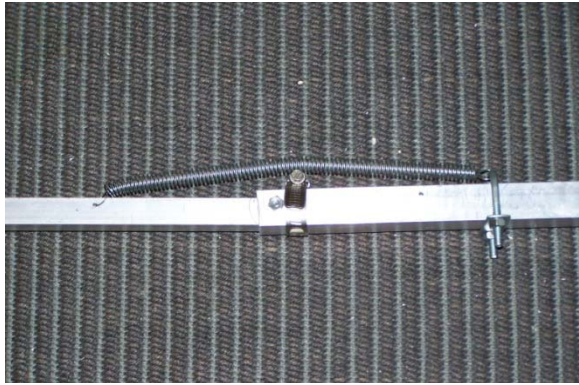


Figure 53 - Completed joint (extended)

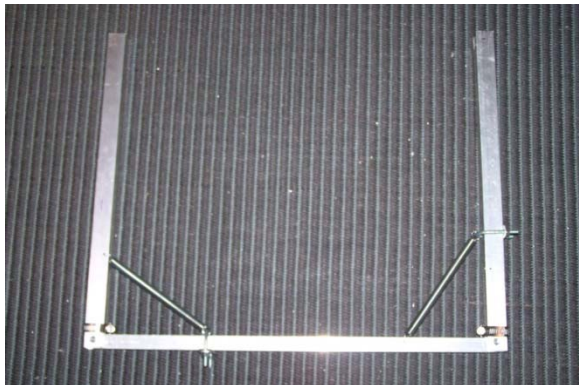


Figure 54 - Completed arm assembly

## Appendix C - Single Probe Test Data

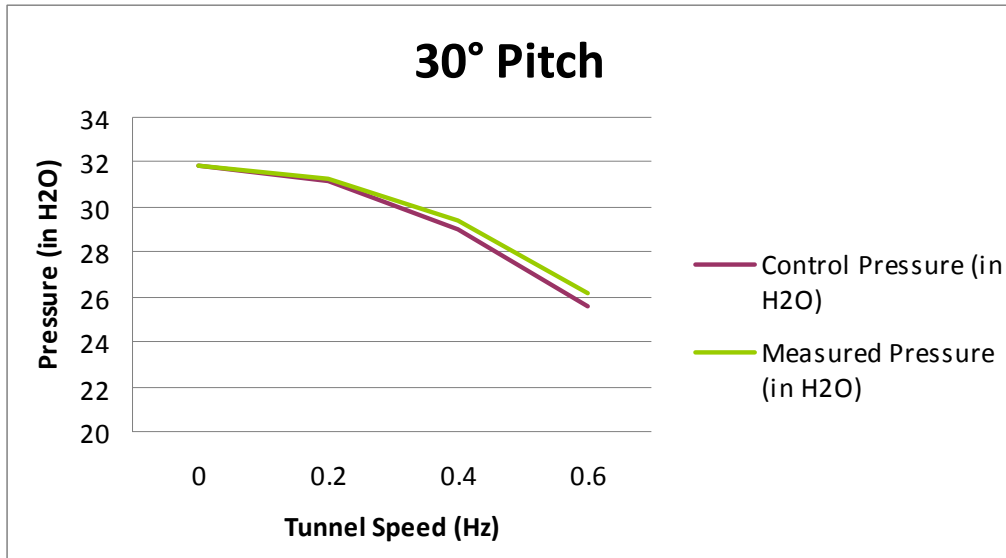


Figure 55 - Test results of single probe at 30° pitch with respect to flow

Table 10 - Test results of single probe at 30° pitch with respect to flow

30° Orientation				
Tunnel Motor Speed (Hz)	0	0.2	0.4	0.6
Control Pressure (in H <sub>2</sub> O)	31.85	31.15	29	25.6
Measured Pressure (in H <sub>2</sub> O)	31.85	31.25	29.4	26.15
Difference $\Delta P$	0	-0.1	-0.4	-0.55
Calculated Windspeed	7.285831	7.216878	7.00	6.601767

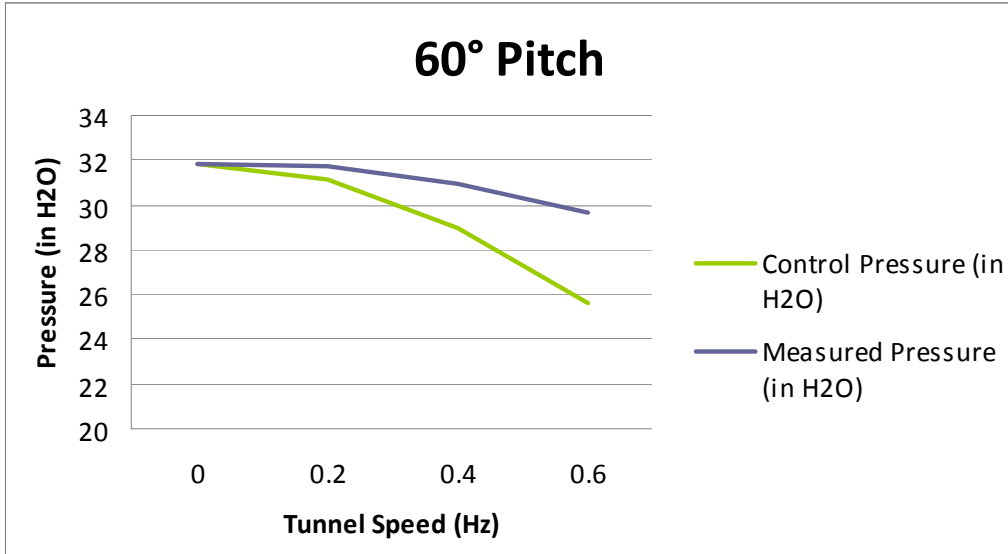


Figure 56 - Test results of single probe at 60° pitch with respect to flow

Table 11 - Test results of single probe at 60° pitch with respect to flow

60° Pitch				
Tunnel Motor Speed (Hz)	0	0.2	0.4	0.6
Control Pressure (in H <sub>2</sub> O)	31.85	31.15	29	25.6
Measured Pressure (in H <sub>2</sub> O)	31.85	31.7	30.9	29.65
Difference $\Delta P$	0	-0.55	-1.9	-4.05
Calculated Windspeed	7.285831	7.268654	7.17635	7.029699



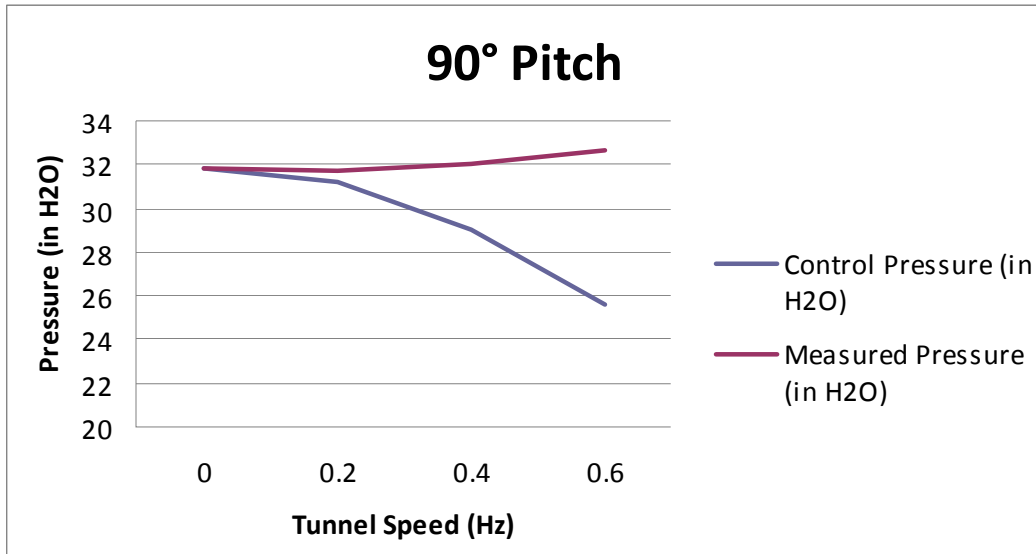


Figure 57 - Test results of single probe at 90° pitch with respect to flow

Table 12 - Test results of single probe at 90° pitch with respect to flow

90° Pitch				
Tunnel Motor Speed (Hz)	0	0.2	0.4	0.6
Control Pressure (in H <sub>2</sub> O)	31.85	31.15	29	25.6
Measured Pressure (in H <sub>2</sub> O)	31.85	31.7	32	32.7
Difference $\Delta P$	0	-0.55	-3	-7.1
Calculated Windspeed	7.285831	7.268654	7.3029674	7.382412

## Appendix D - Full Sensor Package Test Data

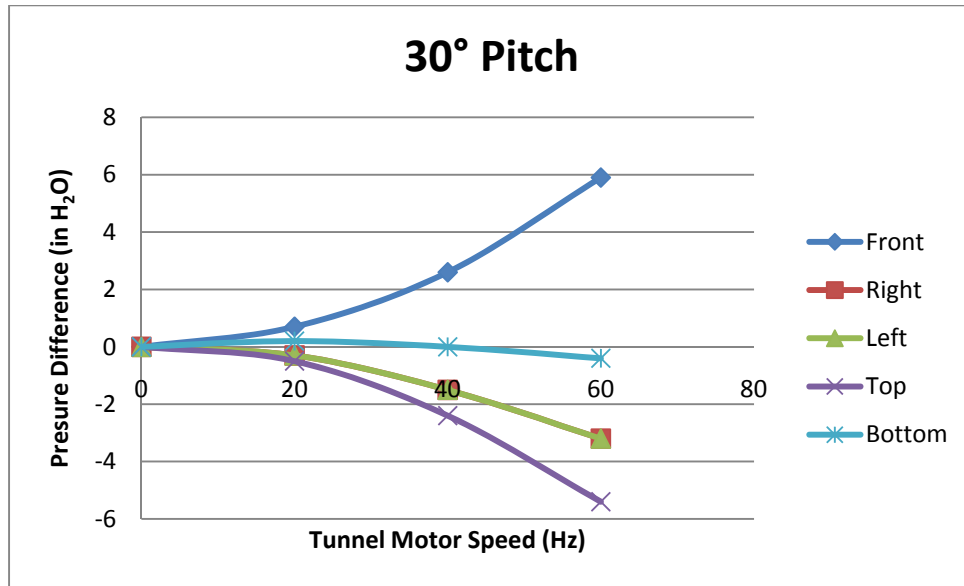


Figure 58 - Test results of sensor package at 30° pitch with respect to flow

Table 13 - Test results of sensor package at 30° pitch with respect to flow

30° Pitch								
Tunnel Motor Speed (Hz)	0		20		40		60	
	Pressure Measurement	Pressure Difference	Pressure Measurement	Pressure Difference	Pressure Measurement	Pressure Difference	Pressure Measurement	Pressure Difference
Front	31.8	0	31.1	0.7	29.2	2.6	25.9	5.9
Right	31.8	0	32.1	-0.3	33.3	-1.5	35.0	-3.2
Left	31.8	0	32.1	-0.3	33.3	-1.5	35.0	-3.2
Top	31.8	0	32.3	-0.5	34.2	-2.4	37.2	-5.4
Bottom	31.8	0	31.6	0.2	31.8	0.0	32.2	-0.4

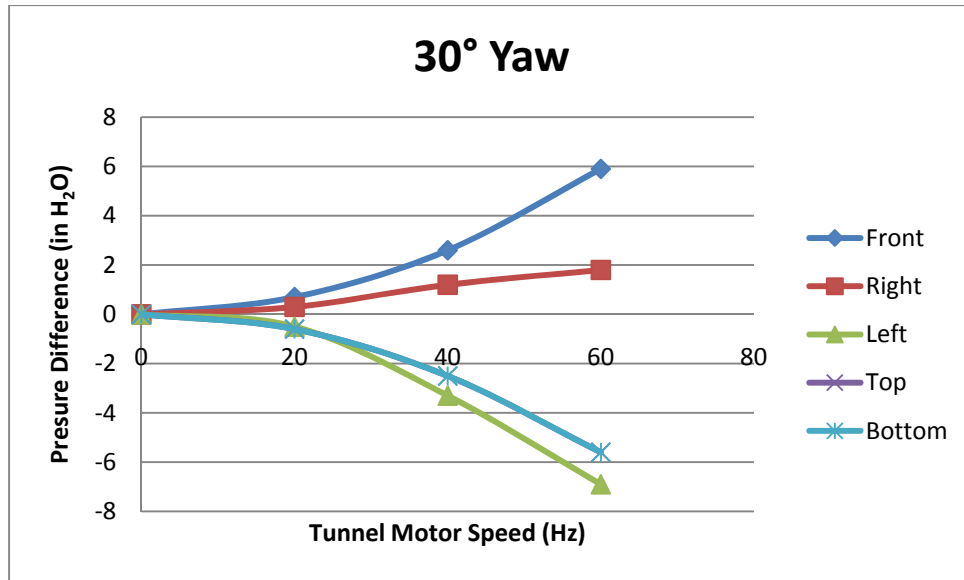


Figure 59 - Test results of sensor package at 30° yaw with respect to flow

Table 14 - Test results of sensor package at 30° yaw with respect to flow

30° Yaw								
Tunnel Motor Speed (Hz)	0		20		40		60	
	Pressure Measurement	Pressure Difference	Pressure Measurement	Pressure Difference	Pressure Measurement	Pressure Difference	Pressure Measurement	Pressure Difference
Front	31.8	0	31.1	0.7	29.2	2.6	25.9	5.9
Right	31.8	0	31.5	0.3	30.6	1.2	30.0	1.8
Left	31.8	0	32.3	-0.5	35.1	-3.3	38.7	-6.9
Top	31.8	0	0	31.8	34.3	-2.5	37.4	-5.6
Bottom	31.8	0	32.4	-0.6	34.3	-2.5	37.4	-5.6

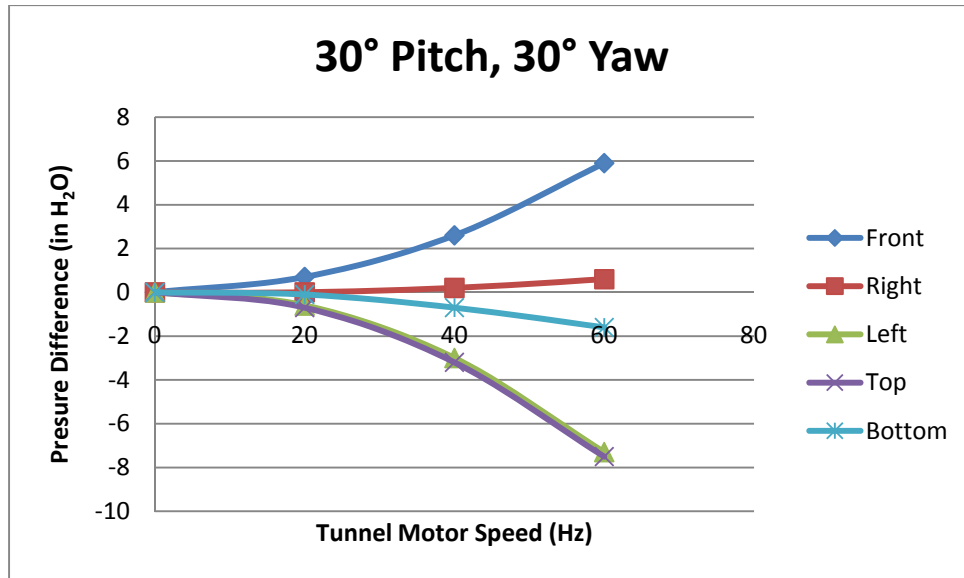


Figure 60 - Test results of sensor package at 30° pitch and 30° yaw with respect to flow

Table 15 - Test results of sensor package at 30° pitch and 30° yaw with respect to flow

30° Pitch, 30° Yaw								
Tunnel Motor Speed (Hz)	0		20		40		60	
	Pressure Measurement	Pressure Difference	Pressure Measurement	Pressure Difference	Pressure Measurement	Pressure Difference	Pressure Measurement	Pressure Difference
Front	31.8	0	31.1	0.7	29.2	2.6	25.9	5.9
Right	31.8	0	31.8	0	31.6	0.2	31.2	0.6
Left	31.8	0	32.4	-0.6	34.8	-3.0	39.1	-7.3
Top	31.8	0	32.5	-0.7	35	-3.2	39.3	-7.5
Bottom	31.8	0	31.9	-0.1	32.5	-0.7	33.4	-1.6

# Appendix E - Data Sheets

## E.i United Sensor Kiel Probes



3 Northern Boulevard, Amherst, NH 03031-2329  
 TEL: 603-672-0909 · FAX: 603-672-0037  
 E-mail: unitedsensor@unitedsensorcorp.com

### KIEL PROBES

#### General Information

##### Aerodynamic Properties

Kiel probes are used to measure total pressure in fluid stream where the direction of flow is unknown or varies with operating conditions. Their correction factor is 0 when used within the ranges outlined below.

##### Mach Number Range

True total pressure is indicated up to a Mach Number of 1.0. There is a slight drop in yaw in sensing range above Mach Number 0.3m. This decreases averages about 4% for all types at a Mach Number of 1.0.

##### Reynolds Number Range

Insensitive to Reynolds Number except at extremely low velocities for Pitot-Static probes. For air this limiting velocity is about 4 ft/sec for the smallest size Kiel probes listed.

##### Time Constant

This depends on the complete installation, probe, pressure lines, and manometer. With 1/8" connecting hose up to 20 ft. long and a liquid manometer of 1/4" ID, the Type B probe will reach equilibrium reading in approximately 15 seconds. Using this time "t" as a standard the other time constants for average stem lengths will be:

Type	Constant
A	2.4t
C,D,H	.04t
E,F	.02t

##### Turbulence Errors

Negligible, especially since the probe is yaw insensitive. Very High turbulence may cut down the yaw and pitch insensitive ranges however.

##### Yaw and Pitch Angle Range

The outstanding advantage of Kiel probes compared with other total pressure probes is complete insensitivity to direction of flow within certain limits. Their yaw and pitch characteristics are generally the same although stem interference on some designs will change one from the other. Fig. 1 shows these flow angles and Fig. 2 is a typical calibration curve of a Type A probe. It can be seen that the correction factor equals 0 up to the limits of the yaw range and then drops very sharply. The range is arbitrarily defined as the point where the error equals 1% of velocity pressure. Symbols used in these figures are:

- Pt: Total Pressure
- Ps: Static Pressure
- Ptp: Indicated Total Pressure

The yaw and pitch range for all types listed above at a Mach Number of .25 are:

Type	Yaw Range	Pitch Range
A	±52°	+47° - 40°
B	±48°	±45°
C	±54°	±49°
D	±54°	±49°
E	±63°	±58°
F	±67°	±61°
G	±31°	±35°
H	±35°	±38°

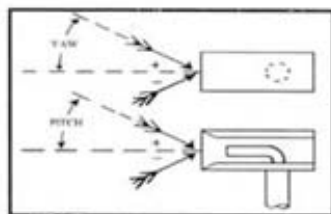


Figure 1. Flow Angles

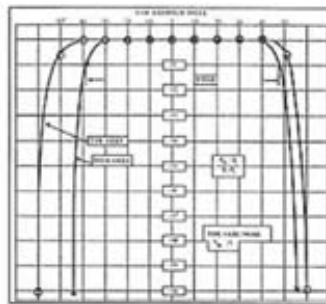


Figure 2. Typical Calibration Curve of Type A Probe

**Boundary Effects**

Boundary effects are small as in all total pressure probes. However, in steep total pressure gradients as near solid boundaries or in "trough" behind guide vanes a shift in the effective center of the probe occurs, so the total pressure measured corresponds to the streamline 0.5d away from the geometrical center of the head in the direction of the higher total pressure as shown in Fig. 3.

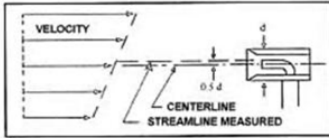


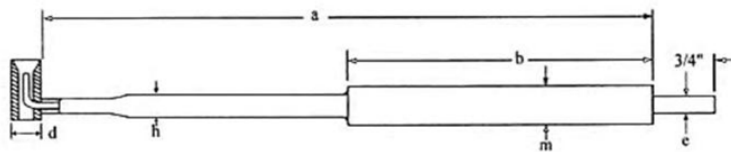
Figure 3. Shift in Effective Probe Center

**Installation**

These probes are usually installed through holes large enough to pass the head as listed on the Kiel Specification pages. See each individual type for the minimum size.

**Special construction including other material, designs to customer's specifications, special take-offs, and mounting adapters quoted as requested.**

**Ordering Information**





- K: Class = K (Kiel) All stainless steel construction
- B: d = See chart and table - Type A, B, C, D, E, F, R
- C: h = 1/8" - see chart for range in each type
 

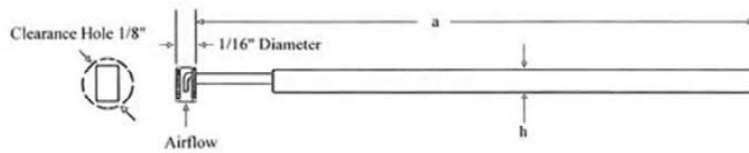
A	C	D	E	F	H	J
1/16"	1/8"	5/32"	3/16"	1/4"	5/16"	3/8"
- 12: a = 12" - Overall length - inches
- F: m = 1/4" - Reinforcing tube diameter (Omit if no reinforcing required)
 

C	D	E	F	H	J	L	M	N
1/8"	5/32"	3/16"	1/4"	5/16"	3/8"	1/2"	5/8"	3/4"
- 10: b = Reinforcing tube length - inches (Omit if no reinforcing required)
- C: e = 1/8" - Take-off diameter (Omit if take-off is same size as stem; i.e. "h")
 

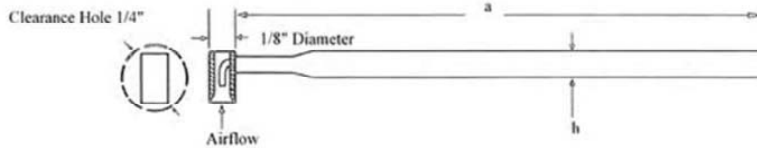
A	C	D	F
1/16"	1/8"	5/32"	1/4"
- W: Standard Braze: Silver soldered for use up to 900°F, this type supplied unless otherwise noted by N or W in suffix above.
- N = High temperature braze for use up to 1,500°F
- W = Welded for use up to 2,000°F >



Ordering Part Number	Sensing Head Description	Probe Diameter h	Probe Length a	Yaw Range **	Pitch Range **	Time† Constant (Sec.)
KAA-"a"	1/16" Dia. Miniature Type KA	1/16"	Standard Probe Lengths are 6", 8", 12", 24"	±52°	+47° -40°	36
KAC-"a"		1/8"				
KBA-"a"	1/8" Dia. Standard Type KB	1/16"		±48°	±45°	15
KBC-"a"		1/8"				
KBS-"a"-W						

Type KA:

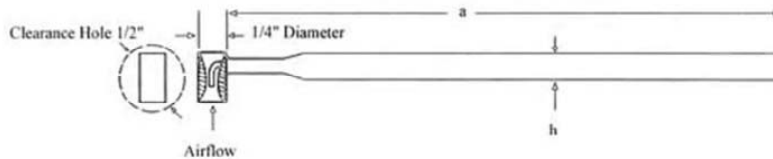


Type KB:

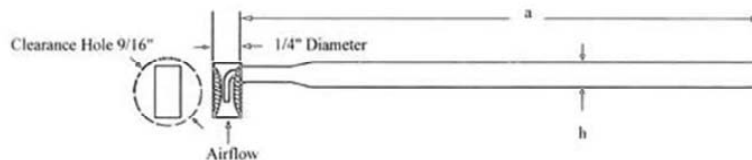



Ordering Part Number	Sensing Head Description	Probe Diameter h	Probe Length a	Yaw Range **	Pitch Range **	Time† Constant (Sec.)	
KCC-"a"	1/4" Dia. Venturi Type KC 	1/8"	Standard Probe Lengths are 6" 8" 12" 24"	±54°	±49°	0.6	
KCE-"a"		3/16"					
KCF-"a"		1/4"					
KCF-"a"-W		1/4"					
KDC-"a"	1/4" Dia. Venturi Type KD 	1/8"		±54°	±49°		0.6
KDE-"a"		3/16"					
KDF-"a"		1/4"					
KDF-"a"-W		1/4"					


Type KC:



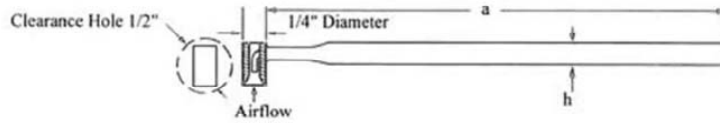
Type KD:



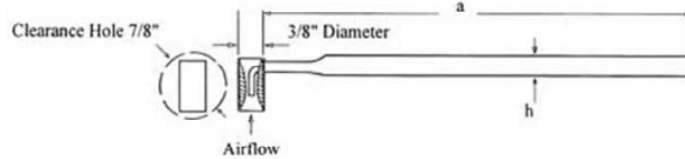
Ordering Part Number	Sensing Head Description	Probe Diameter h	Probe Length a	Yaw Range **	Pitch Range **	Time† Constant (Sec.)
KRC-"a"	1/4" Dia. High Range Type KR 	1/8"	Standard Probe Lengths are 6" 8" 12" 24"	±54°	±49°	0.6
KRF-"a"		1/4"				
KEC-"a"		3/8" Dia. Venturi				

KEE-"a"-W	Type KE	3/16"			
KEF-"a'		1/4"			
KFF-"a"	3/4" Dia. Venture Type KF	1/4"	$\pm 67^\circ$	$\pm 61^\circ$	0.3

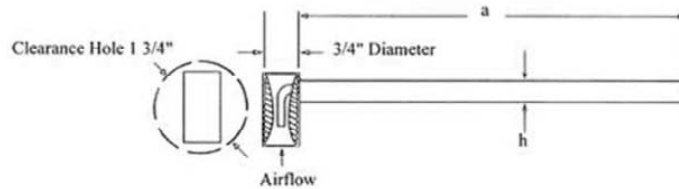
Type KR:



Type KE:



Type KF:



United Sensor Corporation • 3 Northern Boulevard, Amherst, NH 03031-2329 • TEL: 603-672-0909 • Fax: 603-672-0037